Structure of the accretionary complex of Barbados, I: Chalky Mount

R. C. SPEED *Department of Geological Sciences, Northwestern University, Evanston, Illinois 60201*

ABSTRACT

The island of Barbados is underlain by a basal tectonic complex that may be representative of rocks and structures of the structural high of the accretionary prism of the Lesser Antilles arc. At Chalky Mount, the complex consists of six fault-bounded packets of east-northeast strike and steep dips. The packets are composed of deformed but generally coherent Cenozoic sedimentary rocks, terrigenous turbidite in five of the packets and hemipelagic rocks in the sixth. There is no evident stratigraphic affiliation among beds in any of the six packets.

Rocks in fault packets underwent sequential deformations, most of which can be timed as early, contemporaneous, or late with respect to cessation of interpacket motions. Early structures in packet 1 consist of a main fold train with easterly striking axial planes and related thrusts, broken formation, and homoaxially refolded folds. Packet 1 also contains later open folds with northeast strikes. Packets 2–4 are relatively thin slices within a fault complex, the Chalky Mount fault zone, in which late left-oblique slip occurred on two of the four faults of the zone. Packet 5 contains three phases of deformation: an early near-recumbent major fold, marginal belts of fault-related second folds, and open post-fault third folds. Packet 6 includes early folds that are tightened and reoriented toward its northern fault boundary where it is locally a thrust.

Early structures in each packet are the most pervasive and record the major stratal shortening. Shortening in each packet is approximately normal to packet boundaries, and early axes lie in the plane of the boundaries. Packet boundaries are interpreted as surfaces of accretion and early structures as deformations generated during transfer of layer successions from an ocean floor to the front of the accretionary prism. Contemporaneous and post-fault structures are local and are due to displacements during reactivation of faults, mainly interpacket, within the accretionary prism.

Early structures at Chalky Mount developed in the brittle state, apparently with displacements taken up by sliding between grains and along layer boundaries. All structures record distinctly nonmetamorphic environments.

INTRODUCTION

This paper presents a structural study of the accretionary complex of the Lesser Antilles forearc exposed on the island of Barbados (Fig. 1). The island occurs at the structural high, the thickest and probably oldest part of the accretionary prism. Outcrops of the complex are probably representative of the arcward region of the accretionary prism because such rocks extend unmodified at least to maximum well depth, 4.5 km, on Barbados (Baadsgaard, 1960; J. E. Schoonmaker and R. C. Speed, unpub. data). Moreover, their physical properties are compatible with velocities and densities calculated from gravity models of that region (Westbrook, 1975). Thus, the structure of the accretionary complex of Barbados may provide a valid record of the early development and subsequent tectonic adjustments of the Lesser Antilles forearc.

My focus is on geometries, sequences, and conditions of deformation, subjects that are basic to an understanding of accretionary tectonics. The area examined is Chalky Mount and vicinity (Figs. 1, 2), which contains the best exposures on Barbados. The main points are that the Chalky Mount area is underlain by a well-organized series of steeply dipping tectonic packets, the fault boundaries of which can be interpreted as surfaces of accretion. The principal structures within each packet are systematic and continuous and are thought to be a product of shortening during accretion. Postaccretion deformation can be recognized only locally and is generally related to reactivation of earlier faults. Finally, rocks of Barbados have always existed in a shallow, nonmetamorphic environment, indicating that advective circulation within the Barbados prism, if any, has been small. Structural analyses of adjoining areas of the accretionary complex are forthcoming products of this study (D. K. Larue and R. C. Speed, unpub. data; R. L. Sedlock and R. C. Speed, unpub. data).

REGIONAL SETTING

The extensive accretionary prism of the Lesser Antilles forearc is underthrust by the relatively west-moving Atlantic lithosphere (Fig. 1). Geophysical studies indicate that the prism is composed of deformed sedimentary rocks that attain a structural thickness of at least 20 km near the forearc basin boundary and wedge out to the east over as much as 300 km (Westbrook, 1975). The eastern 50 km or more of the prism is a zone of modern and Neogene transfer of strata from ocean floor to prism, both by accretion at the toe and by underplating (Chase and Bunce, 1969; Westbrook and others, 1973; Westbrook, 1975; Peter and Westbrook, 1976; Biju Duval and others, 1978; and Moore, Biju Duval, and others, 1982). More westerly regions of the prism presumably represent earlier phases of growth of the forearc.

The island of Barbados (Fig. 1), the only outcrop of the Lesser Antilles forearc, exposes a three-tiered structure (Speed, 1979, 1981; Speed and Larue, 1982) (1) a cap of autochthonous Pleistocene reefs (Mesollela and others, 1970) that blanket all but about 50 km^2 (Fig. 1), (2) an intermediate zone of one or more nappes of pelagic rocks from which dates of early Eocene to middle Miocene are currently known and which are thought to be allochthonous forearc basin deposits, and (3) a basal complex of deformed layered rocks of probable accretionary origin.

Geological Society of America Bulletin, v. 94, p. 92–116, 14 figs., 2 tables, January 1983.

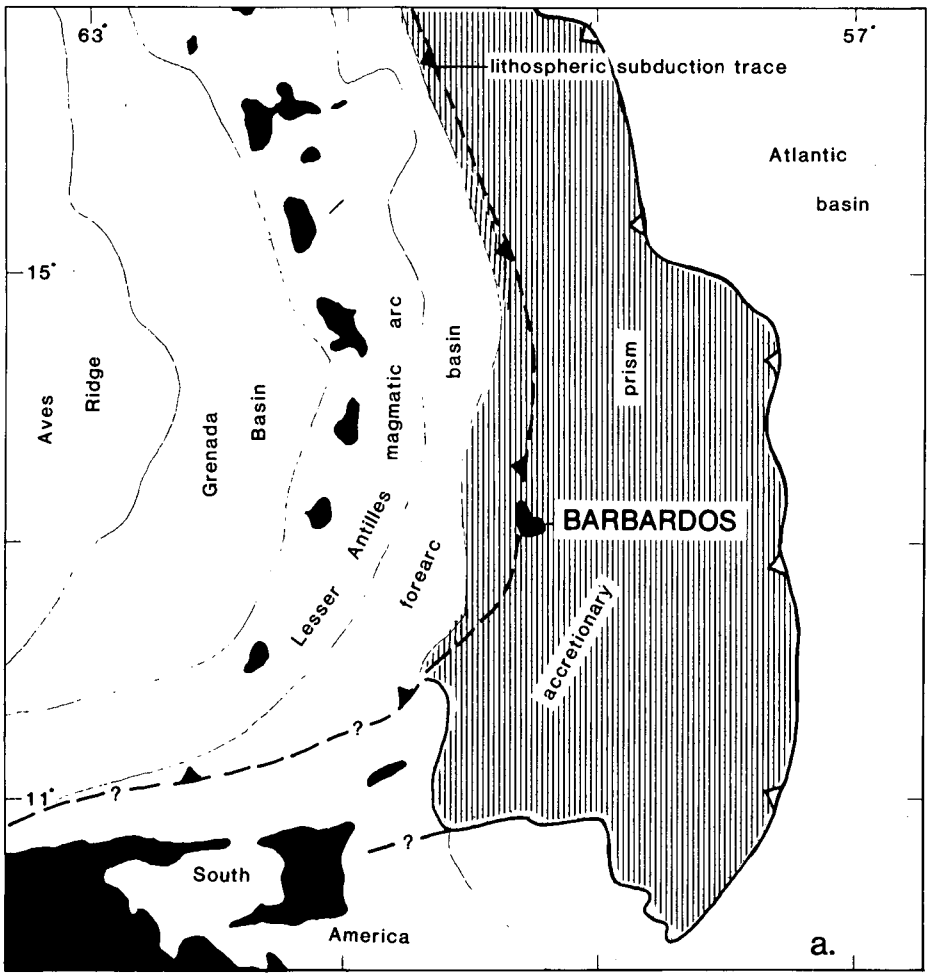

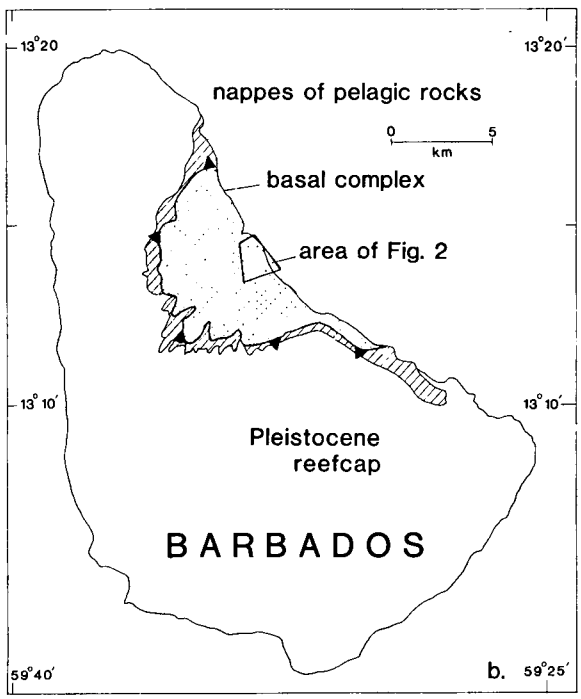

Figure 1. a: regional tectonic units of the southeastern Caribbean; patterned area is accretionary prism of Lesser Antilles arc system. b: map of island of Barbados showing outcrop areas of three major geologic units and location of Chalky Mount area (Fig. 2).

The basal complex was first closely examined by Senn (1940, 1948). He emphasized the organization of a lithostratigraphy among rocks exposed, and customary of the time, he assumed that they were deposited as a continuous succession. Senn's units in what is here called basal complex are the Scotland Formation and the presumably younger Joe's River Formation. They are composed, respectively (Speed, 1981), of terrigenous turbidite and debris flows. These two formations were thought to be overlain by the Oceanic Formation, the pelagic rocks of my allochthonous intermediate tier. New work indicates that each of these lithotypes occurs in discrete fault-bounded packets and that their depositional age ranges are large and overlapping in the Paleogene (Speed, 1979; R. C. Speed, unpub. data). Moreover, another lithic suite, consisting of hemipelagic rocks (radiolarite, mudstone, and quartzose turbidite) of early to late Eocene age, has been recognized in the basal complex. It now seems clear that the pre-Pleistocene of Barbados is a tectonic complex and that the principal lithotypes may never have occupied a depositional sequence. Moreover, there is no basis at present for the assumption that similar lithologies in different fault packets were originally continuous. As a result, the older formational nomenclature is thought to be misleading and has been abandoned.

Several major problems hinder an understanding of the tectonic history of Barbados. One is the paucity of dating of rock deposition, especially of terrigenous lithotypes, within fault packets of the basal complex. Thus, the absolute timing of structural events and stacking orders among accreted packets are poorly known. Second, it is not certain what age span the Lesser Antilles forearc represents. Third is the uncertainty of whether regional rigid rotations have affected orientations of structures of Barbados. Paleomagnetic work in progress may solve this problem (M. Beck and R. C. Speed, unpub. data). Last is the question whether the Barbados accretionary prism has developed fully under the present plate regime or whether it incorporates prisms developed under two or more diversely oriented regimes (Speed, 1981).

GEOLOGY OF CHALKY MOUNT

Fault Packets

The basal complex of the Chalky Mount area (Fig. 2) is composed of six generally

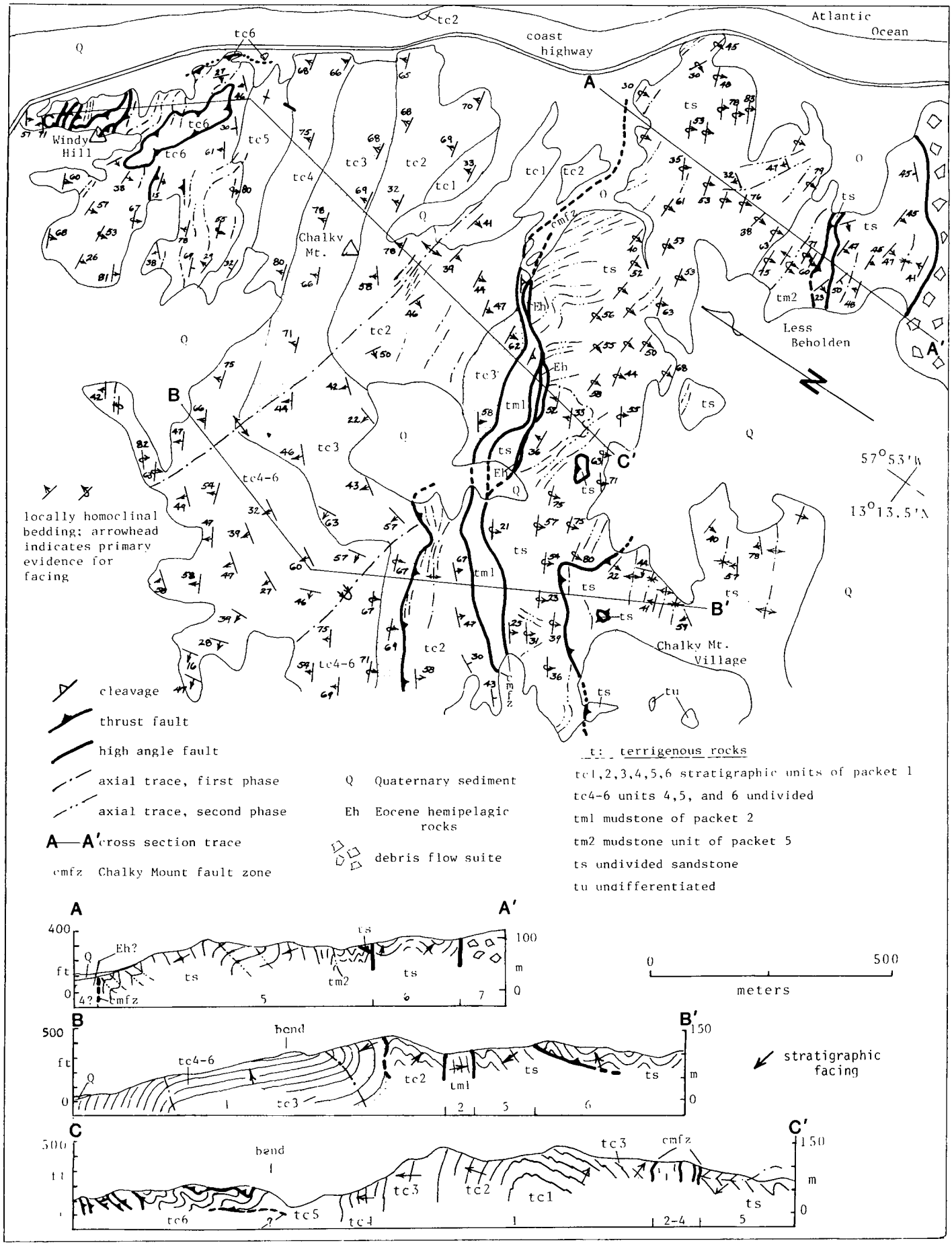

Figure 2. Geologic map and sections of Chalky Mount area; located on Figure 1.

steeply dipping fault-bounded packets of east-northeast strike. Individual packets are indexed by number in Figure 3, and their lithic contents are summarized in Table 1.

The faults that separate packets are identified by discordance of bedding in both walls to the separating surface, by opposed facings of beds in unlike strata, and by abrupt transitions in fold characteristics. Packet boundaries are commonly sharp, but zones of fault-related disruption and flattening or folding exist locally. There are no evident correlations among beds of the six packets. This suggests that displacement magnitudes of the boundary faults are greater than outcrop lengths of the packets (Fig. 2) and lateral dimensions of the varied submarine fan facies that make up five of the six packets.

Packets vary markedly in width, from 10 to more than 100 m. Packets 3 and 4 are thin and lensoid, whereas thicker packets are continuous across the map area. At Chalky Mount and adjacent areas, hemipelagic rocks constitute thin packets, whereas packets of terrigenous rocks are both thick and thin. There are no evident vertical trends in packet configuration in the 200 m of relief in the Chalky Mount area. Packet 6 departs from the basic architecture of vertical stacking because part of its northern boundary is a south-dipping thrust (Fig. 2, section BB'). Juxtaposition of the fault packets occurred generally after strong deformation of the rocks they contain, but at least some of the packets underwent open folding after emplacement.

The minimum age of faulting cannot be directly established in the Chalky Mount area, but it is probably pre-Pleistocene because major packet-bounding faults elsewhere in Barbados (Speed, 1981) do not cut the overlying reef cap. The maximum age of last motions of faults in the Chalky Mount area, indicated by ages of beds they cut, is early middle Eocene to middle late Eocene for the packet 1–2 fault and middle early Eocene for the packet 4–5 fault (Table 1).

TABLE 1. STRATIGRAPHIC AND LITHOLOGIC DATA FOR PACKETS 1–6

Packet	Lithic suite	Map units (Fig. 2) and strat. thickness* (m)	Lithotypes	Depositional age date
1	Terrigenous	tc6 >120?	Massive and graded quartz sandstone in tabular beds 1–10 m thick, interbedded base-present and base-absent turbidite (.01–1 m thick) and ungraded thin-bedded cross- and plane-laminated quartz sandstone; mudstone interbeds as much as 50 cm thick common in parts of section. ss/mst 2-5 in lower two-thirds, ~ 1 in upper one-third	None
		tc5 20–50	Organic mudstone with scattered laminae and thin beds of quartz sandstone; ss mst ~0.25 at base, diminishing upward	None
		tc4 80	Channelized pebbly quartz standstone amalgamated in beds 1–5 m thick that are closely spaced in two successions, each ~25 m thick; rest is base-present and base-absent turbidite (~1 m thick) and massive organic mudstone in layers 1–5 m thick	Resedimented forams and corals indicate maximum age between early middle Eocene and mid-late Eocene (Speed, 1979)
		tc3 130	Massive quartz sandstone in tabular beds 1–7 m thick, chiefly medium- to coarse-grained and plane-laminated, separated by lensoid mudstone ≤3 cm thick	None
		tc2 80	Two upward-thickening cycles of quartzose turbidite culminating in massive quartz sandstone (≤5 m thick); top of unit includes channelized, stratified, locally imbricated conglomerate ~7 m thick	None
		tc1 >25	Dark mudstone, base-absent turbidite, and massive quartz sandstone in beds ≤1 m thick; ss/mst <0.3	None
2	Terrigenous	tm1 >20	Predominant dark, reddish mudstone, intercalated green laminated mudstone, laminae and thin beds of fine-grained quartz sandstone, and 1 m-thick bed of coarse-grained quartz sandstone; ss/mst ~10	None
3	Terrigenous	ts1 >15	Graded and massive quartz sandstone in beds ≤2 m thick, turbidite, minor thin mudstone beds; ss/mst ≥10	None
4	Hemipelagic	Eh >10	Laminated to thin-bedded radiolarian earth and green siliciclastic mudstone with no radiolaria; rare quartz sand as scattered grains and irregular nests in mudstone; local calcareous radiolarian earth beds 1–10 cm thick	Radiolaria in *T. cryptocephala* or *P. striata* zones, early to mid-early to Eocene (W. R. Riedel, 1981, written commun.)
5	Terrigenous	ts2 >350	Chiefly sandstone: thin- to thick-bedded plane-laminated fine- to medium-grained quartz sandstone, massive quartz sandstone 2–8 m thick; interbedded base-absent turbidite and dark mudstone; ss/mst varies between 1 and 5	None
		tm2 >30	Dark siliciclastic mudstone, scattered laminae of quartz sandstone, and thin mud-rich turbidite	None
6	Terrigenous	ts3 >100	Chiefly coarse-grained quartz sandstone commonly rich in solid hydrocarbon in graded and massive beds as thick as 2 m; ss/mst >10	None

*Stratigraphic thicknesses of units tc2-5 are complete; other units are faulted, and preserved thicknesses are minimum.

Lithotypes

Table 1 outlines the lithic constitution of the six packets of the Chalky Mount area and the stratigraphic divisions distinguished in packets 1 and 5. Terrigenous strata, called Scotland Formation by Senn (1940), constitute all but packet 4 and are composed of coarse quartz-rich and pelitic rocks of sub–wave-base, probably deep marine accumulation (Speed, 1979). The terrigenous sediment is of continental provenance, almost certainly from cratonal South America, and was probably deposited in a trench wedge and(or) varied sites in one or more subsea fans. The terrigenous strata are certainly older than the Pleistocene reef cap, but otherwise are poorly dated. In the Chalky Mount area, only coarse resedimented sandstones of unit tc4, packet 1 (Fig. 2), have yielded datable fossils: neritic benthic foraminifera and corals (Alfred Senn collections 102, 165, 167, and 360 *in* Vaughan and Wells, 1945). The ages of such faunas range from Cretaceous (Albian) (Douglas, 1961) to a minimum between early middle Eocene and middle late Eocene[1] (S. H. Frost, 1979, oral commun.; Speed, 1979). Thus, the age of unit tc4 is between early middle Eocene and Pleistocene. The hemipelagic rocks of packet 4 consist chiefly of early Eocene radiolarite and mudstone.

The next four sections present details of the structure of fault packets 1–6 of the Chalky Mount area. They are followed by a general summary of the main structural relationships.

Packet 1

Packet 1 (Fig. 3) consists of a succession of terrigenous strata at least 600 m thick, constituting six stratigraphic units (Fig. 2) that vary markedly in proportions of sandstone and mudstone and in maximum layer thickness (Table 1).

Structures of packet 1 are of four types: (1) soft-sediment deformation features; (2) a pervasive main fold set representing the first tectonic deformation (D1); (3) thrust faults, associated disrupted bedding and folds of phase D1* that developed both early and late in the first tectonic deformation; and (4) superposed open major folds, mainly cryptic, that may represent a discrete second tectonic deformation (D2). Foliation exists only locally as spaced cleavage in mudstone in zones of fault-related deformation, and lineation only as striae on cleavage of certain orientation ranges in such zones. General characteristics of the structures of packet 1 are described below; spatial variations and orientation data, divided among 13 domains, are discussed later.

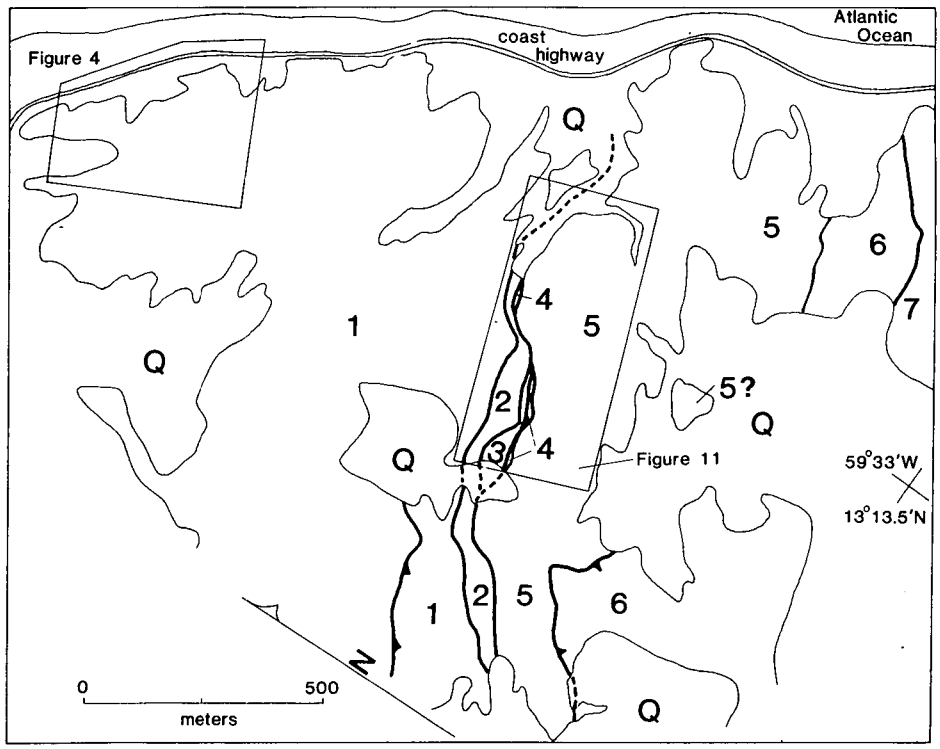

Figure 3. Map showing division of Chalky Mount area into fault packets, each designated by number; Q = Quaternary.

Soft-Sediment Structures

Deformation features within beds, convolute lamination and fluid escape structures, are widespread in sandstone of packet 1, most notably in thick-bedded and pebbly types. Soft-state transfer of material between beds such as ball and pillow structure and intrusions, however, is minor. A few sandstone intrusions have been recognized in units tc4 and tc6; they consist of irregular dikes of coarse, poorly sorted sandstone that cut as much as 1 to 2 m of beds and of thin sills that project from the dikes into finer-grained wall rocks. Source layers of the sandstone dikes are not easily identified, suggesting they were emptied during sand mobilization.

Slumped beds also are apparently rare. One example of a probable slump occurs within channelized strata in unit tc4 (see Fig. 5a, below). A slab of sandstone containing highly disharmonic folds and apparently contemporaneous fluid escape structures lies above a truncation surface and is overlain by an olistostrome about 4 m thick of organic mudstone containing floating blocks of folded sandstone. The olistostrome is succeeded by the depositional base of a series of channel-fill sandstones. Folds in the slumped masses have axes that depart substantially from the clustered orientations of main set tectonic folds. The principal criterion for slump origin of these structures is their occurrence between conformable successions of strata.

In general, however, folding and disruption of beds in packet 1 followed deposition of the entire stratigraphic succession and are of tectonic origin because (1) unconformities cutting D1 and D1* folds and disrupted beds are lacking, (2) main set folds (D1) apparently developed as a coherent train of upright folds with rectilinear axes that involved the entire section of packet 1, (3) periodic intrastratal folds of fluid-escape origin in sandstones are reoriented systematically around folds of the main set, and (4) main set folds of sandstone beds are almost entirely of parallel type and were probably cylindrical over substantial lengths before second deformation. Points 3 and 4 indicate

[1] *Neodiscocyclina anconensis* (Barker), *Siderastrea scotica* Wells, and *Goniopora hedbergi* Wells.

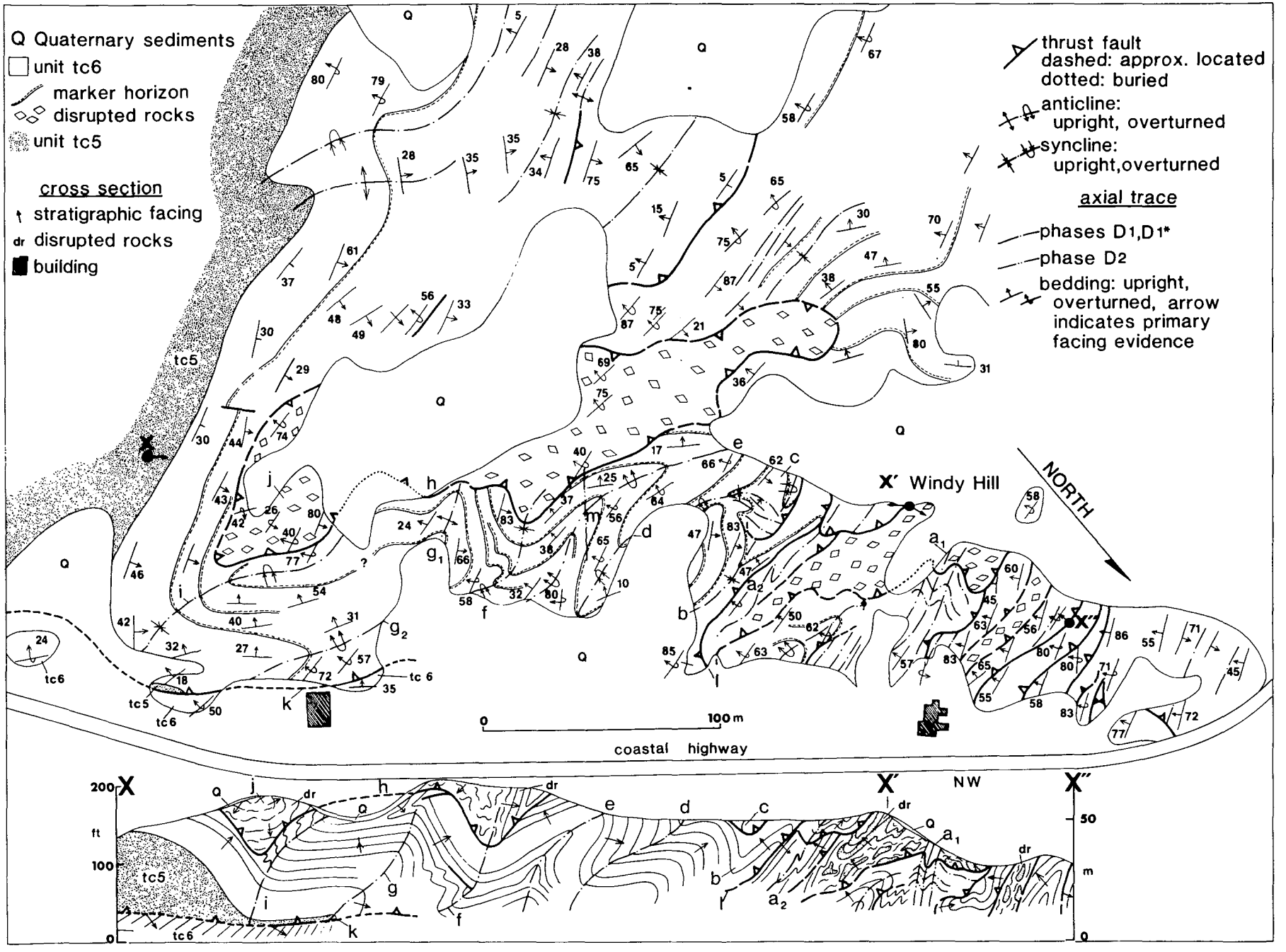

Figure 4. Geologic map and section of part of Windy Hill area in northern fault packet 1; located on Figure 3.

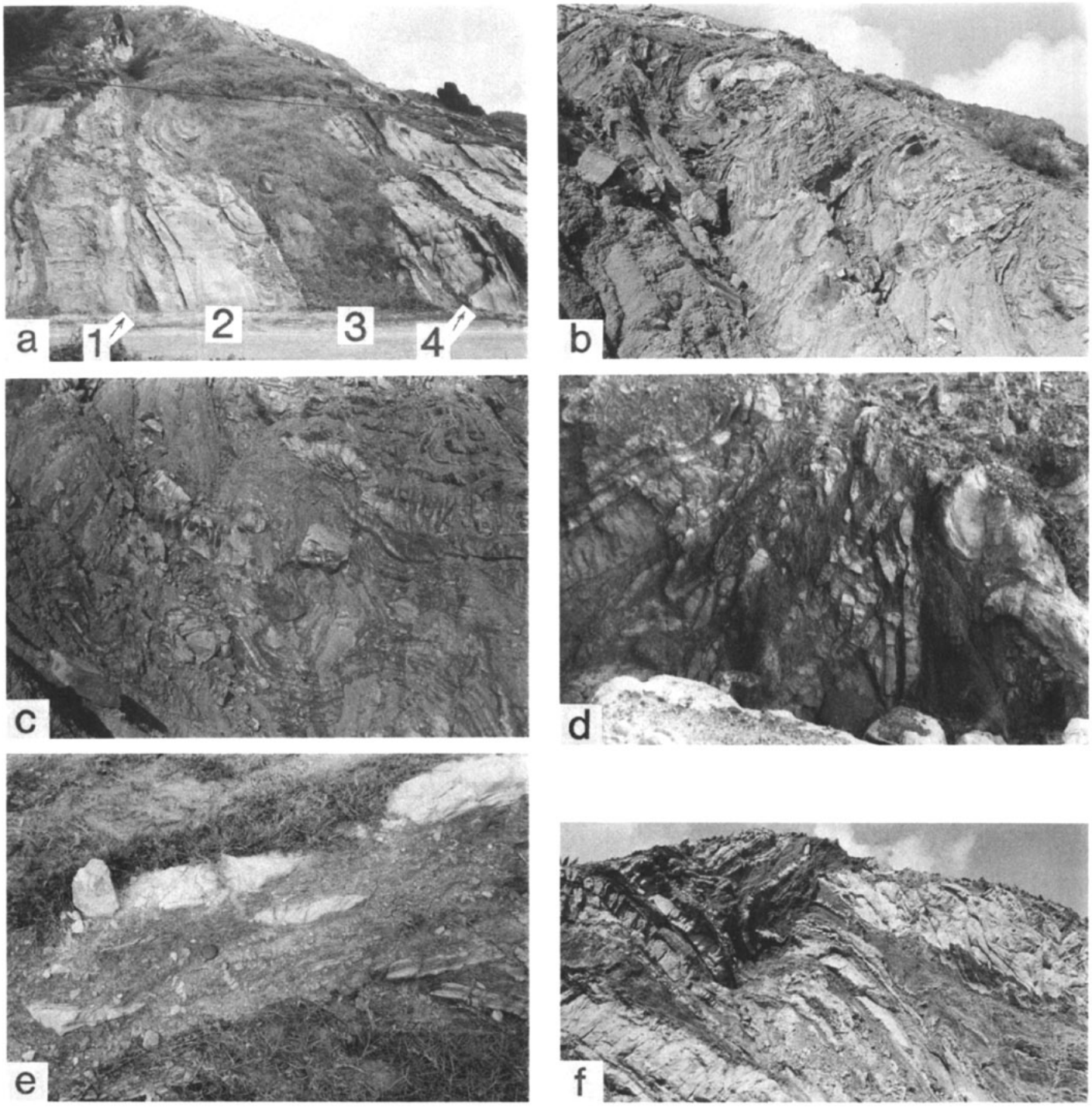

Figure 5. a: probable slumped rocks within units tc4, packet 1: 1 = slump base, 2 = slumped sandstone with discordant base (left) and top, 3 = mudstone with sandstone blocks, 4 = base of succeeding strata; width of outcrop at road level about 20 m. b: broken formation, domain 1a, packet 1; broken folds of sandstone beds in matrix of poorly cleaved mudstone and less disrupted thin-bedded sandstone; thick bed segment at lower right 1.5 m thick. c: broken formation, domain 1a, packet 1; disruption of thick sandstone beds, thin beds more continuous; width of field about 3 m. d: broken formation, domain 1d, packet 1; strongly disrupted beds and folds of sandstone in mudstone with well-developed spaced cleavage; width of field 3 m. e: broken formation, north wall of packet 2 within 5 m of packet 1–2 boundary; aligned but dispersed phacoids of sandstone in cleaved mudstone; tabular block faces and cleavage are parallel; disk is 4 cm in diameter. f: transition from coherent strata of domain 1c to broken formation of domain 1d, packet 1; beds at upper left are inverted and in nearly recumbent fold with beds in lower right; thick sandstone (2.8 m thick) in upper right cut by inverted fold limb; see Figure 8b.

that intrastratal deformation and folds of the main set formed sequentially and that sandstones were sufficiently consolidated to maintain orthogonal layer thickness during main set folding. D1* disrupted rocks differ from slumps by their occurrence in fault-bounded slices or nappes that have no conformable boundaries and by the general colinearity of D1* fold axes with those of main set folds. The existence of girdled axes in slump folds has been widely noted (Woodcock, 1976).

Main Fold Set (D1)

The main fold set consists of a train of close to tight folds between 1 and ≥500 m wide with generally east-striking and south-dipping axial surfaces. The folds are either upright or overturned to the north, but the major folds of the set are too large to offer confidence of vergence direction. Traces of axial surfaces of larger folds of the main set are shown on maps and sections in Figures 2 and 4. The nonplanarity of axial surfaces is interpreted as due to homoaxial refolding during progressive main set deformation and to open refolding in a discrete second phase (D2).

Wavelengths of the main set are closely related to stratal thickness. The broadest exposed fold is an anticline, ≥500 m wide, defined by the form surface of unit tc3 (Fig. 2, sections BB′ and CC′) which is a composite of thick sandstone beds totaling about 130 m thick. Multilayer units (tc2, tc4, and tc6) that contain thick and thin beds (Table 1) have fold widths between 1 and 60 m and apical angles between 22° and 105°, averaging about 60°. Sand-rich beds are folded with near-parallel style, whereas mud-rich interlayers are commonly in classes 1c and 3 (Ramsay, 1967). Single surface shapes of folds in multilayer units are visually estimated to range from chevron to sinusoidal (Hudleston, 1973). The two predominantly mudstone units, tc1 and tc5, contain tight folds, mostly ≤2 m wide, defined by laminae and thin beds of sandstone.

Measurements of layer lengths over half-wavelengths or greater indicate shortening between 30% and 42%, thus providing a range of minimum values for compressional strain. There are no foliations associated with main set folds.

Thrusts, Folds, and Disrupted Rocks (D1*)

Packet 1 includes local thrusts, folds, and disrupted rocks that are discordant to the main D1 fold train but were probably generated during the same deformation phase. The alliance is drawn by the geometric and kinematic compatibilities between them and D1 folds. The local structures include imbricated thrust slices and discrete thrust nappes. In one place, a nappe of broken folds developed before or during incipient main set folding. At another, similar structures were generated late in main set folding. The local structures include folds that are deformed by main set folds, folds that deform main set folds, and folded folds in which it is not clear whether D1 is the earlier or later phase. The main affiliation among all these folds is their homoaxiality.

Because the local structures did not form at a single time and because many cannot be placed in a time series, I class them simply as D1* structures. The protracted generation of local structures during the main deformation indicates it was progressive and inhomogeneous.

Disrupted rocks in packet 1 generally occupy fault-bounded slabs, either in imbricate zones or in a discrete nappe. Rocks in zones of disruption can be correlated with continuous beds in packet 1, generally those where medium- or thick-bedded sandstones occur with relatively thick mudstone interlayers. Disrupted rocks consist of blocks of sandstone 0.1 to 10 m long in a matrix of cleaved mudstone. The blocks commonly can be related to original strata, and, within individual bodies, facing of sandstone blocks is generally uniform. No exotic fragments have been recognized. These properties indicate that disrupted rocks of packet 1 are probably tectonically broken formation, not a sedimentary deposit.

Structures of broken formation vary systematically, probably with respect to the magnitude of deformation. The simplest type consists of rectangular blocks of thicker sandstone beds or hinges of folded sandstones with fractures mostly normal to bedding (Fig 5b). Such fragments commonly retain a rude original stratigraphic ordering (Fig. 5c). Cleavage is spaced, anastomosing (Powell, 1979), and bedding parallel or megascopically obscure in mudstone in simple broken formation. More complex broken formation (Figs. 5d, 5e) consists of lenticular blocks (but rarely in true boudinage), lack of stratigraphic ordering of sandstone blocks, and well-developed spaced cleavage. Microlithon thicknesses are between 0.5 and 3 mm. Cleavage parallels major block faces but is deflected near block tips and is commonly folded where blocks converge or show systematic rotations. In general, intersections among cleavage and between cleavage and block faces are colinear.

Discussion of individual broken formation follows in sections on domainal structure.

Superposed Second Folds (D2)

An apparently discrete second phase of folding in packet 1 is recognized with certainty only in domains 1b and 1c (Fig. 4). There, late folds are open to close and have steeply dipping, northeast-striking axial planes. Cryptic major folds of this generation may be widespread and account for azimuthal variability of main set fold orientations.

Cataclasite Bands

Sandstones throughout packet 1 are locally cut by quasi-planar fractures that contain variably comminuted quartz. The fractures are identified by their blue-gray hue. These cataclasite bands are commonly 0.1 to 1 cm thick, spaced at least 1 m apart, and offset stratigraphic markers no more than a few centimetres. Their concentration increases near packet-bounding and other faults. The bands indicate that, at some stage of deformation, sandstones took up displacements by shearing across grains. Unfortunately, the timing and slip directions of cataclasite bands are unknown.

Windy Hill Ridge

The northern quarter of packet 1, mainly the well-exposed east face of Windy Hill Ridge, provides the most information on relationships of D1, D1*, and D2 deformations and so is discussed in detail. Figure 4 is a large-scale map and section of Windy Hill Ridge. Orientation data (Fig. 6) are divided among five structural domains, 1a–1e: 1a and 1d consist of variably disrupted rocks of D1 and D1* phases, 1c and 1e of beds in mainly coherent folds of the main set (D1), and 1b of a D2 fold.

A thrust (Fig. 4, k) of possibly major displacement is exposed at the base of southern Windy Hill Ridge. Its importance stems from the possibility that rocks of Windy Hill Ridge, indeed, of the entire Chalky Mount area, could be far-traveled with respect to its lower plate. Good correlation of beds in the inverted sequence below

thrust k with those of unit tc6 above, however, implies the fault is intrapacket and has a northwestward component of transport of the upper plate of about 100 m. The attitude and net slip direction are unknown. I speculate that thrust k originated late in the progressive D1 deformation by failure of strongly overturned limbs in the main set fold train.

Domain 1a. Domain 1a (Fig. 6) consists of a series of south-dipping thrust slices, 1 to 25 m thick, that underlies the main continuous succession of Windy Hill (domains 1b, 1c, and 1e) at fault ℓ, Figure 4. Although beds in domain 1e contain a lower proportion of sandstone relative to mudstone than elsewhere in unit tc6, they are included in that unit because distinctive sandstones can be correlated on opposite walls of fault ℓ and across a few other thrusts in domain 1a. From this, I infer that domain 1a is a zone of imbricate slices of the highest beds of unit tc6 and that the thrusts are intrapacket and displaced older over younger strata.

The slices are variously tabular, wedge-shaped and rootless, and folded. Relations shown in Figure 4 indicate sequential development of some adjacent faults. Most slices contain coherent strata in whole or faulted folds, whereas some include mainly homoclines, either upright or inverted. Two slices consist of disrupted rocks or broken formation. Moreover, domain 1a contains the only closely refolded minor folds in packet 1 (Fig. 4, folds a1 and a2). Both generations of folds in domain 1a are called D1* because it is not clear which, if either, is contemporaneous with main set D1 folds of domains 1c and 1e.

Figure 6a gives orientation data for minor folds of beds that evidently are not refolded. Almost all axes plunge shallowly between south and west, and poles to axial planes form a diffuse partial girdle about the mean axis. The correspondence is evident of attitudes of first axes in domain 1a with those of main set folds in domains 1c and 1e (Figs. 6c, 6g), whereas axial planes are more girdled in domain 1a than in the others. Folds verge northward, and all are upward-facing except where inverted by second folds. The length over which attitudes are constant is but a few metres. Data from six subdomains, each about 10 m^2, indicate orientation ranges nearly as great as those of the domain as a whole. The changes are probably due to open second folds allied to those described below, but also to rotation among fragments of broken folds within the slices of disrupted rocks (data included in Fig. 6a). There is no evident difference in the mean and range of axis orientation between broken folds and those in little disrupted slices, whereas the range of dips of axial planes is greater in more disrupted rocks.

Second folds of D1* are nonpervasive in domain 1a but can be seen at sites a1 and a2, Figure 4. At a1, the second folds deform

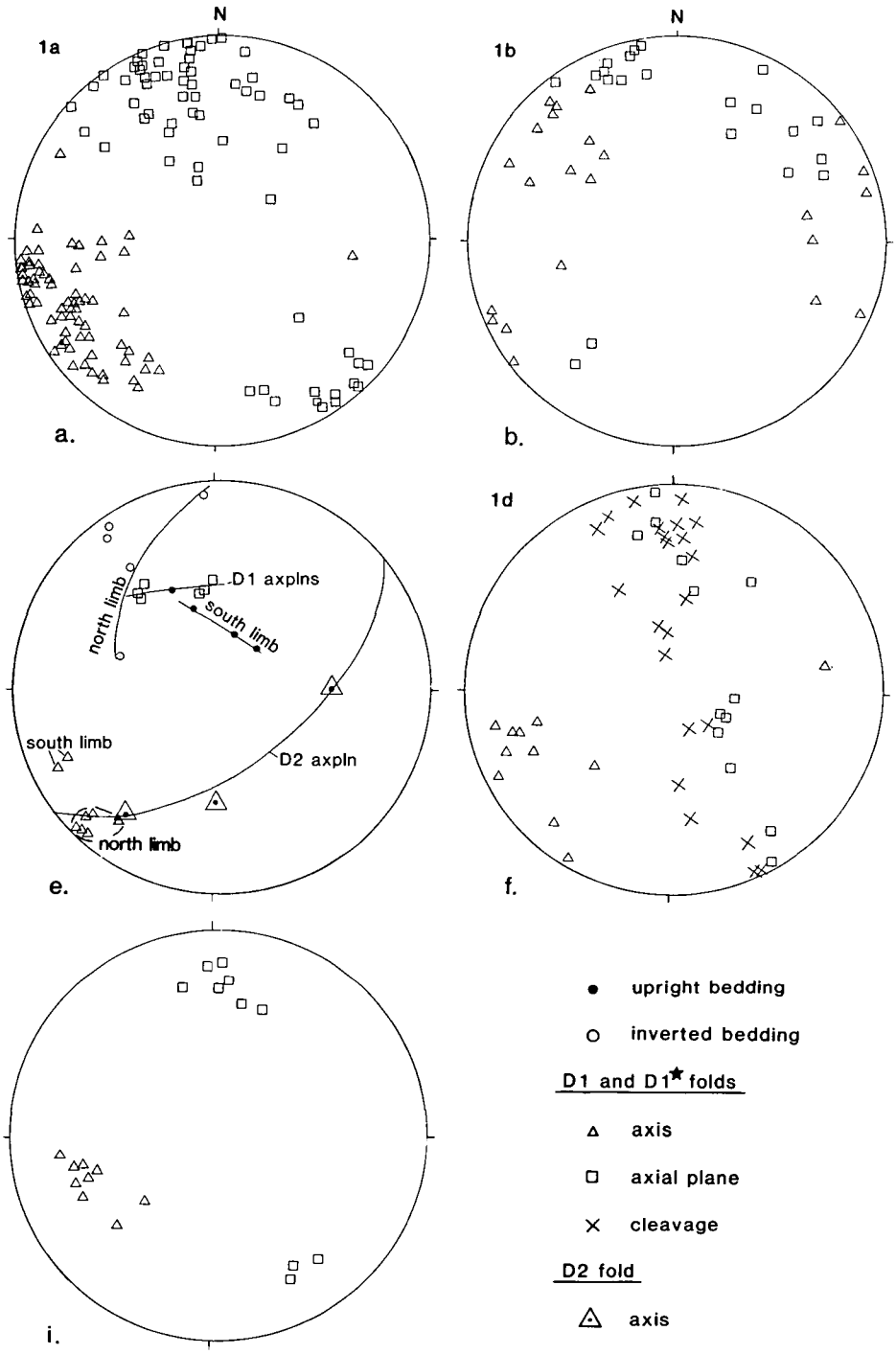

Figure 6. Fold orientation data for domains 1a–e of fault packet 1, Windy Hill area; c: tie lies connect poles of axial planes of individual D1 folds deformed in D1* phase; d: data for phase D2 fold m (Fig. 4); i: minor folds in domain 1e within 3 m of thrust contact with disrupted rocks of domain 1d; equal area net, lower hemisphere used on this and all subsequent fold data plots.

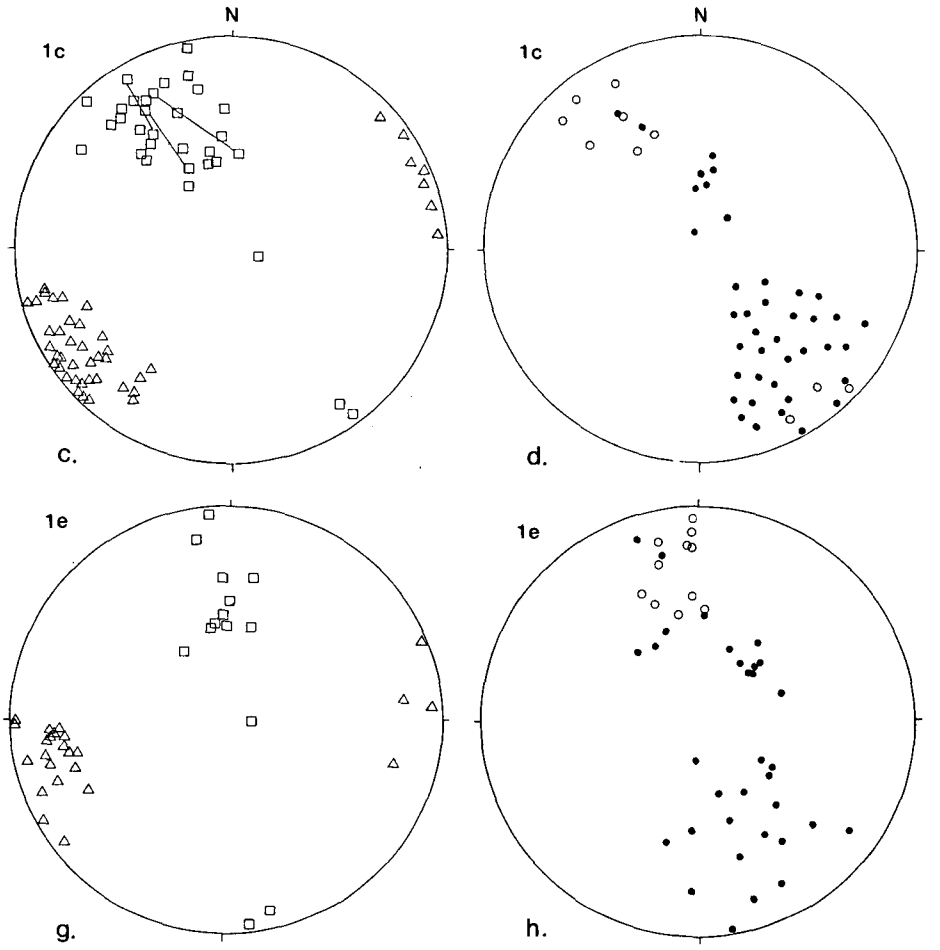

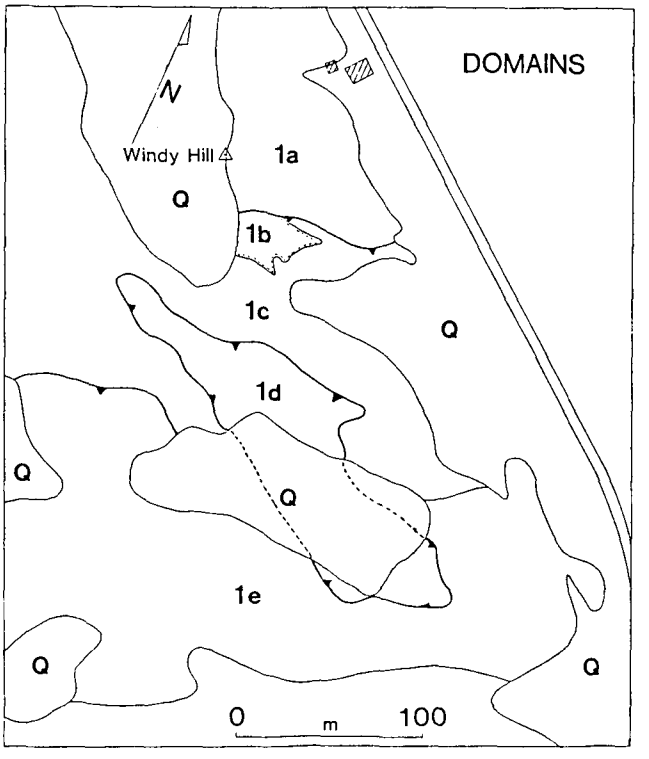

Figure 6. (*Continued*).

both first folds and thrust slices, indicating the second folds are younger than at least some thrusts. Second folds of beds at a1 and a2 (Fig. 7) have interlimb angles between 45° and 90°. First folds are inverted on the northerly limb of the second folds, indicating northward vergence. The folded first folds are strongly disharmonic, and although mudstone in such folds underwent substantial migration, foliations developed in neither phase. Orientation data for refolded minor folds (Fig. 7) indicate that the second axes are nearly colinear to one another, to the majority of first axes of the folded folds, and to the cluster of D1* axes away from second folds (Fig. 6a). The strong homoaxiality of first and second folds is violated by three first axes of the fold shown in Figure 7a; for these, no simple rotation pattern emerges, and they must be explained by displacement incompatibility in the hinge regions (Ramsay, 1967, p. 546). Poles to axial planes of first folds form a partial girdle that is approximately coplanar with that of minor folds away from the refolded folds (Fig. 6a). The axial planes of the second folds dip steeply south-southeast like the mean axial planes of unrefolded minor folds in domain 1a (Fig. 6a) and those of D1 folds in domains 1c and 1e (Figs. 6c and 6g).

The foregoing data indicate that the sequential fold sets of domain 1a were probably generated in a single noncoaxial deformation with clockwise rotation about a fixed southwest-plunging axis. The sequence implies early thrust imbrication and shortening by folding, then locking up of one or more thrusts, and continued folding, all with a component of clockwise simple shear and a north-northwest trend of shortening. It is not clear, however, whether thrusting in domain 1a was early or late in the main deformation. If early, the second folds are probably contemporaneous with D1 folds elsewhere in packet 1. The thrusts, however, could also represent brittle failure of asymmetric D1 folds such that the second folds formed late in the main deformation.

Two thrust slices in domain 1a are composed exclusively of broken formation. Both have abrupt transitions with adjacent slices of mainly coherent beds and were broken before emplacement. Some other slices in domain 1a are increasingly disrupted toward their boundaries, but this seems not to be the case with the broken formation slices. Fragments of folds with full hinges (Fig. 5b) occur near the top of the southern broken formation, but else-

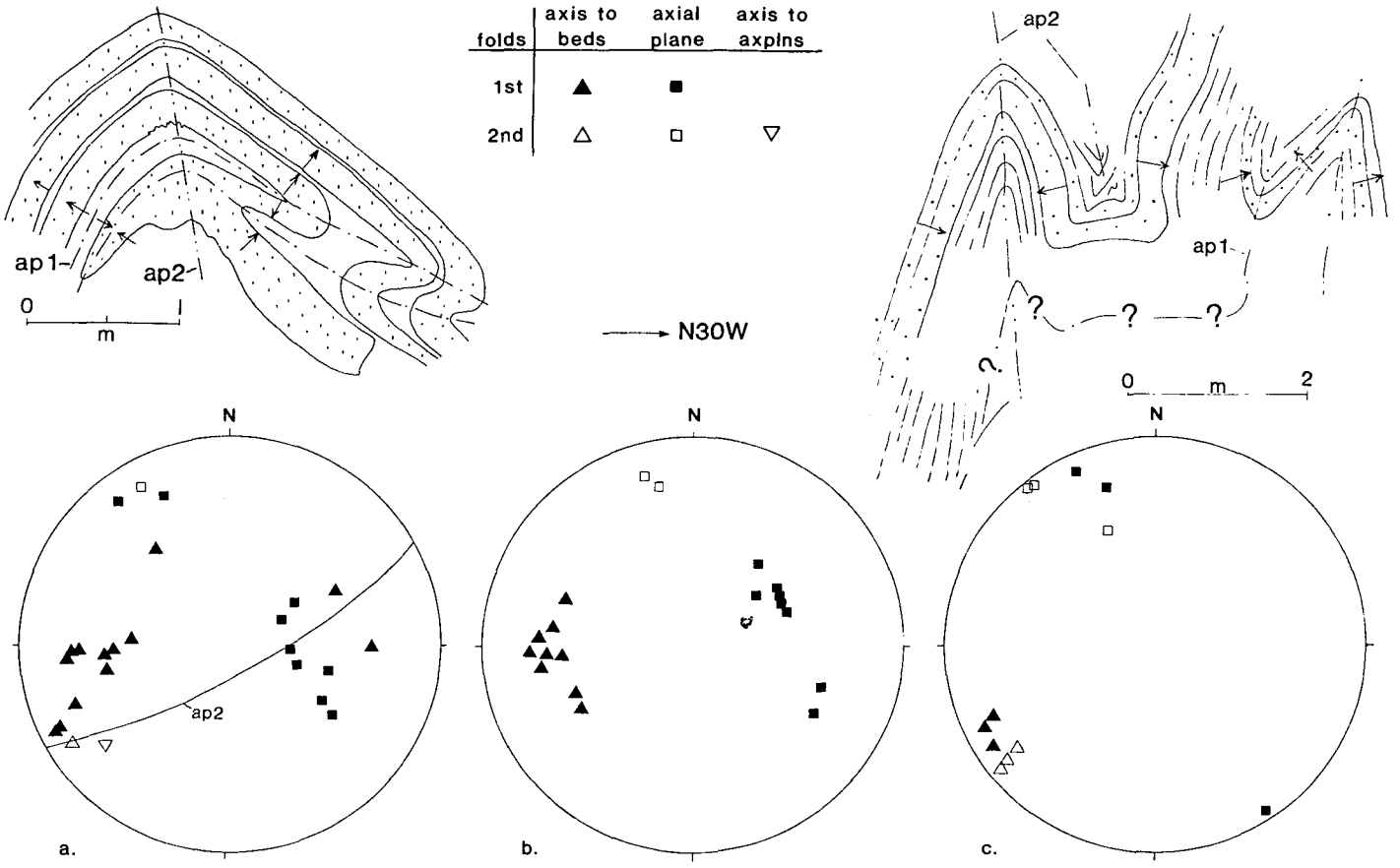

Figure 7. Superposed folds of phase D1*, domain 1a of fault packet 1, Windy Hill area; a: sketched profile and orientation data for an individual folded fold at a1, Figure 4; b: orientation data for minor (first) folds and major (second) folds near a1, Figure 4; c: sketched profile and orientation data for folded fold at a2, Figure 4.

where, the slices of disrupted rocks consist mainly of upright sandstone blocks, many with partial fold hinges a quarter-wave or less in width. This indicates that asymmetric folds in the now-disrupted rocks generally faulted across the intermediate limbs before they grew beyond trivial amplitudes. As noted above, folds in slices of disrupted rocks are homoaxial with other folds in domain 1a and have only a slightly greater rotation of axial planes than undisrupted folds. Second folds at site a1, Figure 4, fold a slice of broken formation. Thus, broken formation in domain 1a has undergone much the same kinematic history as rocks in adjacent slices except for the apparently more pervasive internal faulting that dismembered and variably displaced sandstone beds from their initial horizons.

Domain 1b. This small area contains major and minor folds of the main set that are reoriented in a major fold assigned to phase D2 and are partly broken by south-dipping thrusts (Fig. 4, C; Fig. 6, domain map). Beds of domain 1b lie conformably above those of domain 1c and are bounded on the north by a thrust (ℓ, Fig. 4).

The form of the D2 fold is defined by the deflection to a northerly trend of axial traces of D1 folds as they pass from domain 1c to domain 1b. Orientation data for domain 1b (Fig. 6b) include two subsets: (1) folds of beds that adjoin domain 1c that have typical attitudes of the main set (east-northeast–striking axial planes and west-southwest– and east-northeast–plunging axes), and (2) folds of beds away from the domain boundary that have anomalous orientations (northwest-striking axial planes and northwest– and east-southeast–plunging axes). Folds of the two subsets are continuous, not superposed, and have no differences in geometric character. The axis to the D2 fold is vertical to steeply southwest-plunging, as indicated by the partial girdle of poles to D1 axial planes. D1 axes may occupy a small circle or ellipse about the D2 axis. Comparing fabrics of domains 1b and 1c (Figs. 6b, 6c), it is evident that reorientation of folds in domain 1b was at least partly by clockwise rotation of D1 folds. The D2 axial plane can be only rudely estimated to strike northeasterly and dip steeply from the imprecise axial trace and D2 axis. However, the validity of this attitude is indicated by the existence of a late open major fold (Fig. 4, m) nearby in domain 1c that seems to belong to the same D2 wave form as the fold of domain 1b. The axial plane of fold m strikes northeast and dips steeply southeast (Fig. 6e).

The thrust that is the northern boundary of domain 1b is contemporaneous with or younger than D2 folding in domain 1b. If it is contemporaneous, a component of right-lateral slip on the fault is implied by the orientation of the D2 fold.

Domains 1c and 1e. These domains (Fig. 6) contain mainly coherent beds that are deformed by major and minor folds of the main set (D1). The two domains are divided by an arbitrary boundary, and their stratigraphic sequence is continuous with subjacent units of the Chalky Mount succession.

Major folds of the main set (Figs. 6c, 6g) have axial surfaces that strike northeast to east and dip between 85°SE and 35°SE (Fig. 4). Axes plunge shallowly with an average trend of S60°W and a range of trends of about 50°. Poles to bedding, divided by facing, are displayed in Figures

6d and 6h. Minor folds are rare and are mainly related to décollement within the folded succession. Homoaxial deflections of axial planes occur in all the major folds (Fig. 4, d–g, i), and the open superposed folds are assigned to phase D1*. The D1* axial planes evidently strike east-northeast, but their dips are unresolved.

A differently oriented late major fold (Fig. 4, m) assigned to phase D2 is superposed on main set fold e (Fig. 4). The late fold openly deforms the limbs and axial surface of the D1 fold over a halfwavelength ≥20 m. Figure 6d shows orientation ranges of the three folded surfaces. The two limb distributions are reasonably cylindrical, indicating that the D1 fold limbs were locally planar before later deformation. Orientations of the D1 axial planes are more varied, probably due both to difficulty of measurement and to initial variability. Axes to the three folded surfaces indicate the second axial plane strikes about N50°E and dips about 60°SE. The apical angle of the D2 fold is ≤120°. Axes of the folded main set fold are in two subsets that correspond to the two limbs of the D2 fold. Although the angular difference is small, the pattern of D1 axes suggests rotation about a steep axis. The fabric of D1 axes and poles to axial planes of domain 1c as a whole (Fig. 6c) contains a range in trend and strike like those of D1 elements in the D2 fold. Thus, the azimuthal ranges of data in Figures 6c and 6g may be accounted for by widespread gentle or open D2 folds of which fold m and the late fold of domain 1b are the only resolved examples.

Domain 1d. A folded thrust nappe of partly disrupted beds constitutes domain 1d (Figs. 4, 6). The main features of the nappe are that it is folded by D1 folds, contains broken folds of mainly inverted facing, and was locally derived and underwent northerly transport.

The nappe of domain 1d cuts subjacent beds at small angles except for steep ramps across thick sandstone at h, Figure 4, and beds near j, Figure 4. At both ramps, there is a thin zone of apparently transitional structures between the nappe and its autochthon (Fig. 4). At site h, the zone consists of north-verging, nearly recumbent minor folds (Fig. 5f) of thin beds that lie stratigraphically below the thick sandstone of domain 1c at the crest and northern limb of anticline g, Figure 4. The overturned limbs of the minor folds lap across the truncation of the massive sandstone and grade into the overlying nappe of domain 1d by progressive disruption. At site j, the transitional zone contains broken and refolded minor folds.

The nappe has marked lateral variations in degree of disruption. Its southern two-thirds consists of strongly dismembered sandstone beds, all inverted. Where sandstones were interbedded with mudstone, the blocks are well dispersed in a cleaved mudstone matrix (Fig. 5d). Cleavage is axial planar to the disrupted inverted folds and is locally tightly folded in crenulations that have east-northeast–striking axial planes. The strongly disrupted rocks grade north to fractured steeply inverted beds, and farther, to continuous beds in upright folds (Fig. 4).

Rocks of domain 1d can be related to beds in the lower one-third of unit tc6. Nappe transport was north-northwest as much as 150 m, as indicated by bed correlations, structures in the transitional zones, and fold axis trends (see below).

Axes of minor folds in both disrupted and coherent beds in domain 1d and the intermediate zone (Fig. 6f) are oriented like those of adjoining domains and of the main fold set throughout packet 1. The main distinction is the more complete girdle in domain 1d of poles to axial planes and associated cleavage than elsewhere in packet 1. Moreover, the full range of orientations occurs in subdomains no more than a few metres wide. The variability exists chiefly among individual inverted folds, both within and between discrete blocks. There are no pervasive superposed minor folds in domain 1d that cause the axial-plane variability.

The nappe is clearly deformed by folds f and i of the main set (Fig. 4). The D1 folds are approximately homoaxial with the minor folds within domain 1d (Figs. 6c, 6f, 6g). Rotations of at least 90° among axial planes in domain 1d were evidently caused by the D1 folds, but the rotations cannot be distinguished in the data of Figure 6f because the variability of axial-plane orientations of the minor folds is so local.

The northward emplacement, minor folding, and disruption of rocks in the nappe of domain 1d clearly preceded growth of the main fold set, at least beyond a stage of very low amplitudes. Because the nappe transported locally derived beds, its minor folds must have been generated during nappe motion. However, the parallelism of axes and of shortening trends (bearing of horizontal component of normals to axial surfaces) in folds of the nappe and those of the main set argues that the two fold sets were kinematically related. Therefore, the nappe probably represents local thrusting and associated folding and disruption early in the first (D1) tectonic deformation.

Figures 8a and 8b give a model of the evolution of domain 1d and the local transitional zone to domain 1c. During incipient deformation that led to the main fold set, a south-dipping thrust developed, but initially only in the massive sandstone. The thinner beds below the massive sandstone responded ductilely and took up early displacement by folding in a shear zone that was continuous with the fault in the sandstone. A thrust or series of thrusts ultimately propagated down through the deformation zone, leaving a carpet of truncated north-verging overturned minor folds in the lower plate (domain 1c). As the upper plate rode over the ramp created by the broken end of the autochthonous massive sandstone, the inverted limbs of minor folds cut off from the early deformation zone were folded, then broken in correspondence with a possible change from shortening to extension on crossing the ramp. The model concludes with major folding of the autochthon and the nappe together. The model does not explain why the beds in the northernmost part of the nappe are not disrupted, because they too should have encountered the ramp.

An alternative evolution to that of Figure 8 would start a major recumbent fold pair, the higher one north-closing, then develop a thrust through the intermediate limb. It is rejected because early minor folds, which should have developed widely at the time of hypothesized recumbent folding, are absent except for those of the transitional zones.

Domains 1f and 1g. These two domains laterally divide the outcrop belt of the mudstone-rich unit, tc5, (Figs. 2, 9). The only recognizable structures in unit tc5 are folds of sandstone laminae and beds, most of which are ≤3 cm thick. Cleavage is absent. The folds are tight, long-limbed, and largely dismembered, so that asymmetry is indeterminate. The distribution of axes (Figs. 9a, 9b) is like that of the main fold set elsewhere in packet 1, except for the greater range in trend of west-plunging axes and predominance of north-dipping axial planes in unit tc5. The origin of the domainal difference in plunge is not evident but may be related to a cryptic major D2 fold with axial trace near the domain boundary.

Domains 1h, 1i, and 1j. The major anticline-syncline couple of the main fold set can be traced laterally by the form surfaces of units tc3 and tc4 through domains 1h-j (Fig. 9). The anticline is upright and has an apical angle of about 120°. The syncline is overturned to the north and its southern limb is cut by an intrapacket thrust that raised lower strata in the south wall (Fig. 2). The apical angle of the syncline is ≤80°. Asymmetry of the major couple is indeterminate.

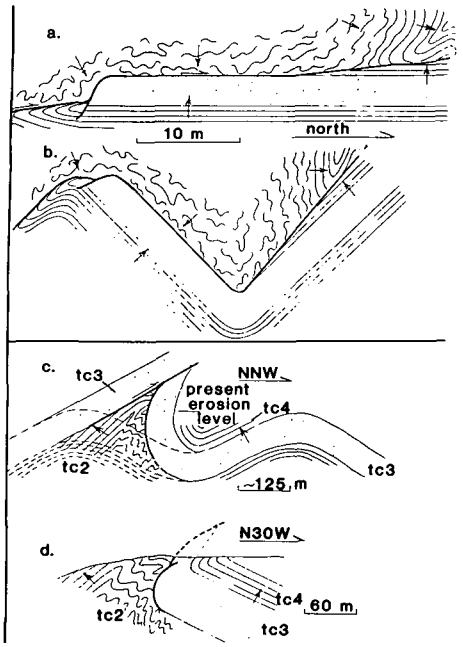

Figure 8. Some thrust-fold relationships in fault packet 1. a: model section of thrust nappe of domain 1d before significant limb appression of D1 folds; b: nappe of domain 1d after D1 folding; c: model of fold-thrust evolution in domains 1j and 1k; dashed lines show fold form before thrusting and solid lines show structures after thrusting; d: sketch of present relationships of broken formation and folds in unit tc2 of domain 1k (Fig. 9) to major syncline of unit tc3 (domain 1j, Fig. 9).

Domain 1h (Fig. 9c) includes the northern limb of the major anticline and several minor folds in discordant sandstone bodies that are probably slumps. The slump folds have axes of variable orientations. Domain 1i (Fig. 9d) contains the northeast-striking intermediate limb of the major folds and a few southwesterly plunging minor folds of the main set, and domain 1j (Fig. 9e) includes bedding of the overturned southern limb of the syncline but no minor folds.

The accuracy of orientations of major fold elements in domains 1i and 1j is open to question because of difficulty in measurement. The azimuthal range of axis trends between west-northwest and south-southwest is particularly suspicious because there are no systematic differences between the two folds or changes with position along their axial traces. The consistent west-northwest strike of the axial surfaces, however, is real and differs by 20° to 40° from strikes of axial planes in eastern packet 1. The east-west orientation differences may indicate the existence of a cryptic gentle D2 fold with northeast axial trace in the eastern third of packet 1.

Domain 1k. Domain 1k encompasses a tract of unit tc2 that lies south of the major fold couple of domains 1h-j and is faulted against higher beds that constitute the south limb of the major syncline (Fig. 2, section BB'). The fault surface is curved about strike and dips variably south and north more or less conformably with attitudes of massive sandstone in the north wall, as sketched in Figure 8d. Rocks of domain 1k are cut out to the southeast by the Chalky Mount fault zone.

The major structure of domain 1k is an anticline, ≥30 m wide, upright to overturned, and north-verging (Figs. 2, 9f). The south limb is homoclinal, whereas the hinge region includes abundant minor folds with steeply north- or south-dipping axial planes. The north limb is locally homoclinal and upright or steeply overturned, but elsewhere it is deformed in D1* folds. Where rocks of domain 1k are structurally above the northern fault, deformation of the north limb created coherent tight minor folds that commonly have shallowly dipping axial surfaces. Where rocks of domain 1k are below the fault, folds and beds are disrupted but have attitude ranges similar to those in the hinge region of the major anticline of domain 1k (Fig. 8d).

Although rocks of domain 1k are in a fault-bounded slice, their tectonic fabric (Fig. 9f) is much like that of other domains containing multilayers, such as domain 1e. Thus, it may be concluded that folds of domain 1k away from the northern fault contact belong to the main set of packet 1. D1* deformation in the fault wall is evidently superposed on folds of the main set and consists of (1) homoaxial rotation of minor folds of the main set and (or) second homoaxial, nearly recumbent minor folds and (2) disruption of beds and folds of the main set without rotation. The spatial difference of the two types of structures in the northern fault wall of domain 1k (Fig. 8d) suggests that rocks of unit tc2 in domain 1k flattened and distended against unit tc3 where the fault dips below tc3 and underwent rotational strain where unit tc2 overrode tc3. The main fold set in domain 1k and the fault at the northern boundary of the domain, however, were probably related tectonically because both record the same north-northwest shortening trend.

Folding and Thrusting in Domains 1i–k. A model explaining relationships between folds and the thrust in domains 1i-k, illustrated in Figures 8c and 8d, is as follows. At the onset of main set folding, beds of domain 1k lay below massive sandstone of unit tc3 in the next anticline south of the existing major syncline. During or after folding, this conceptual anticline was faulted, allowing its south limb to be thrust north and overturning the south limb of the existing syncline. The overriding limb of unit tc3 has been eroded. The subjacent, chiefly thin-bedded rocks of unit tc2, however, were driven against the autochthonous limb, riding up and over its upper, overturned regions but flattening and disrupting in extension against its lower hingeward regions.

Domains 1ℓ, 1m. Domain 1m (Fig. 9h) contains rocks of units tc1 and tc2 in the deeply eroded eastern core of the major anticline of the main fold set. Domain 1ℓ (Fig. 9g) lies to the west along the axial trace of the same fold and contains beds of unit tc2 and, on the south flank, unit tc3 (Fig. 2, section CC'). In these domains, the major anticline is upright, has an apical angle of about 90°, and is ≥500 m wide. Minor folds vary in width from 1 to 20 m and in apical angle, 30° to 80°. Single surface shapes vary between chevron and sinusoidal (Hudleston, 1973). In domain 1m, minor folds occur mostly on the south limb and in the hinge region of the major anticline. The larger minor folds are consistently of Z asymmetry, whereas smaller ones are Z or S as appropriate to their position on the larger.

Figure 9h shows that minor fold axes and poles to axial planes in the two domains are moderately clustered and oriented like those of main set folds in domains 1c and 1e (Fig. 6). There is no evident geographic pattern to these data within or between domains. Orientations of local homoclinal bedding in the two domains form a generally cylindrical pattern about the average minor fold axis. Except for a couple of stray points, the data of Figure 9h indicate that only a single deformation can be resolved and that fold orientations in domains 1ℓ and 1m are rectilinear along axial trace.

Packets 2–4

Packets 2–4 are narrow, east-northeast-striking, steeply dipping fault-bounded tracts between the more extensive packets 1 and 5 (Fig. 3, and see Fig. 11, below). Their markedly different lithotypes are described in Table 1. The network of faults that separates and bounds packets 2–4 is called the Chalky Mount fault zone (CMFZ, Fig. 2). The CMFZ and fault-related structures in its walls are considered below.

Packet 2

Terrigenous mudstone-rich packet 2 is nearly pervasively deformed in the eastern

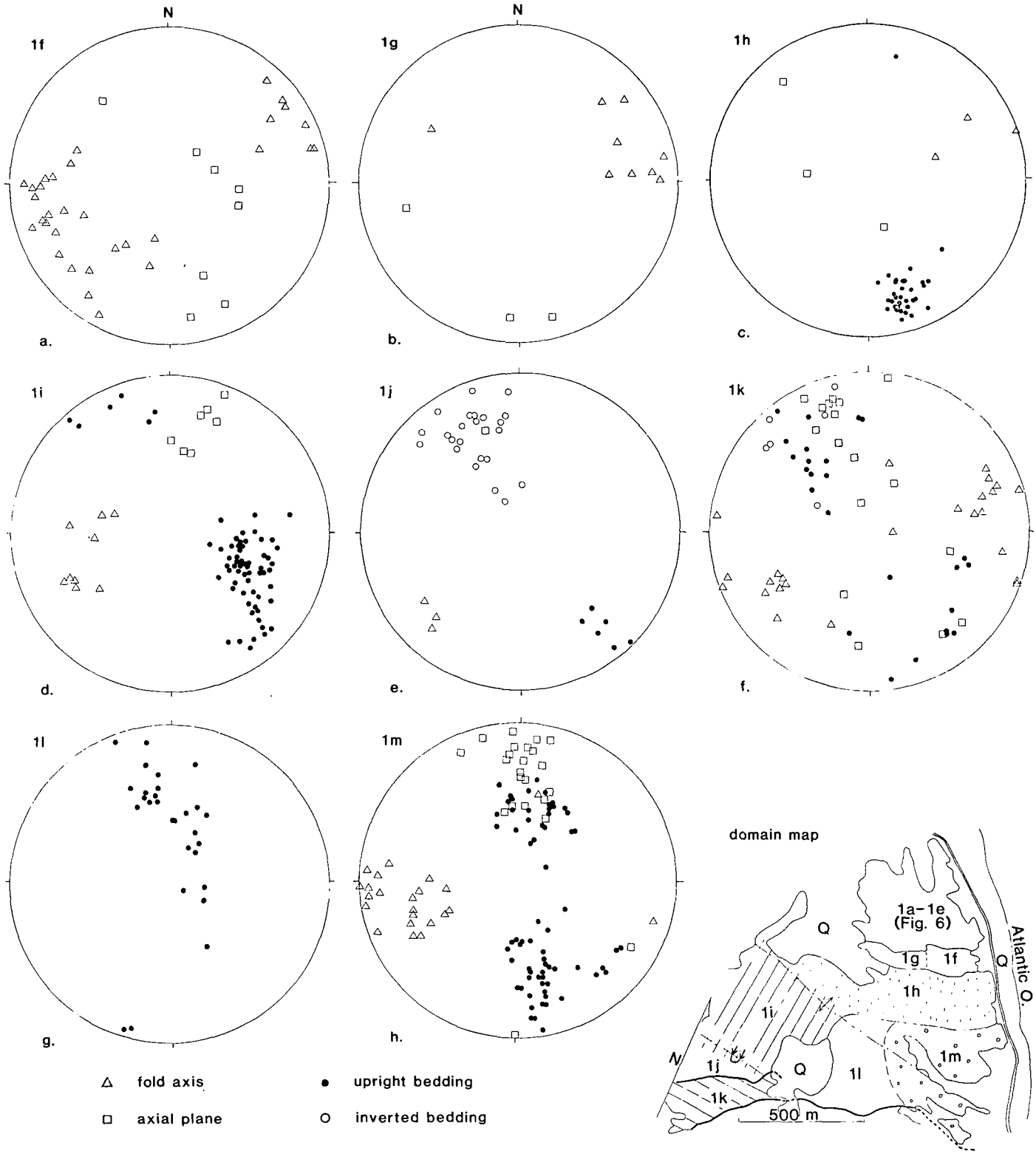

Figure 9. Fold-orientation data and map of domains 1f to 1m, fault packet 1.

one-half of its outcrop belt (see Fig. 11, below). Sandstone laminae and thin beds are in tight, segmented folds; isolated homoclinal beds can be identified as fold limbs by opposing facing. A single thick sandstone bed is openly folded and slightly broken and forms a traceable horizon. Mudstone has a variably developed spaced cleavage and microlithons 0.1 and 1 cm wide. Cleavage is commonly parallel to bedding and can be differentiated from fissility only in the hinge regions of folds. Figure 10a shows axes of folds of bedding and poles to bedding in packet 2 away from marginal zones of fault-related deformation. The distribution of bedding orientations mimics that of cleavage.

Two postcleavage deformations exist in eastern packet 2. One consists of a series of open folds of packet 2 and the Chalky Mount fault zone. These folds have axial

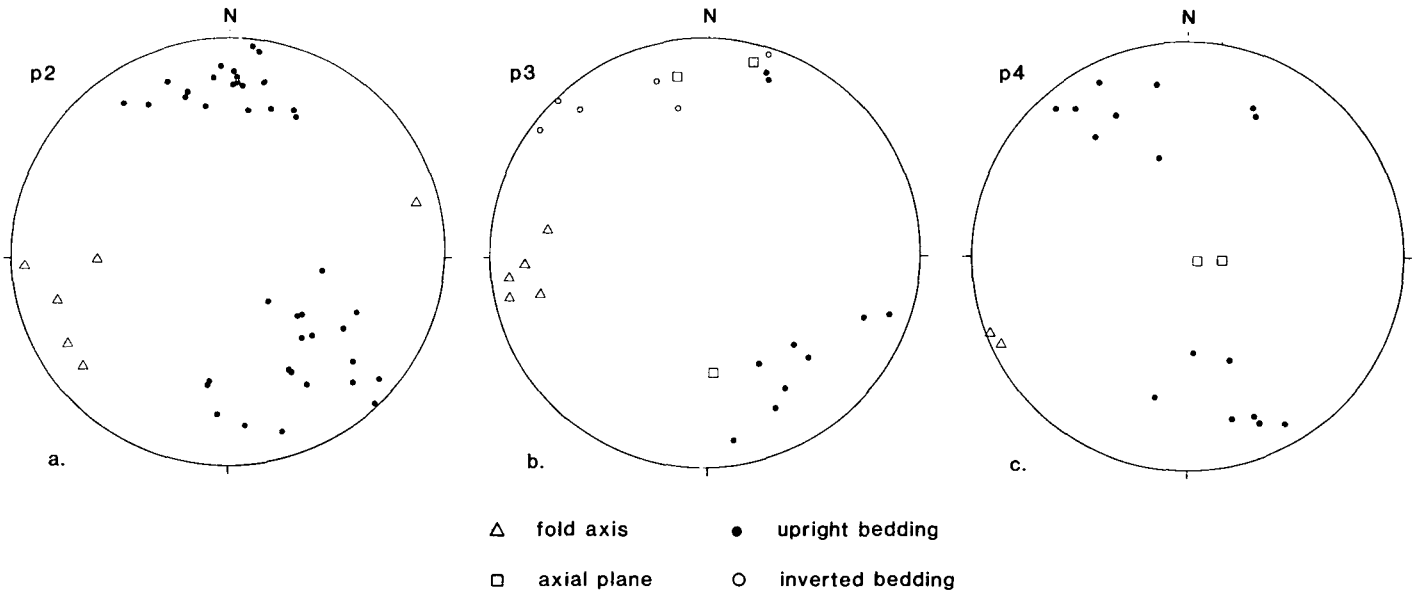

Figure 10. Fold-orientation data for fault packets 2, 3, and 4 (Figs. 3 and 11)

traces (Fig. 11) that trend approximately northwest and cause rotation of elements of Figure 10a, including cleavage, about a vertical to near-vertical axis. The late open folds are allied with a third phase of deformation in packet 5. The other younger deformation feature consists of scattered microfolds of cleavage. Axes of the microfolds (not shown in Fig. 10a) are distributed in an east-west girdle that approximates the average cleavage orientation.

The sparsely exposed western one-half of packet 2 differs from the eastern by its lack of cleavage and by the constancy of facing of its beds. The lesser deformation may be due to the greater parallelism of the northern strand of the CMFZ and bedding in packet 2 in the western than the eastern half.

Packet 3

Packet 3 is a discontinuous slice of sandy terrigenous beds folded in west-plunging, north-verging folds (Fig. 10b) where the packet is thin and in an upright anticline of box form where it is thickest (see Fig. 14e below). It is not clear whether the box fold is primary or whether the southern limb is deformed due to movement on the fault between packets 3 and 4.

Packet 4

Packet 4 consists of laterally discontinuous bodies of hemipelagic rocks (Table 1) no thicker than about 10 m. Contacts with adjacent packets are generally steep and sharp (see Fig. 14b below), and the near-vertical bedding of packet 4 is commonly discordant to both packet walls. Only two minor folds were observed, both gentle and with near-horizontal axial planes (Fig. 10c). Cleavage is absent in packet 4, and radiolaria apparently are not deformed. There is a correspondence in the fabric of packet 4 and adjacent packets in the existence of shallowly west-southwest–plunging axes. The azimuthal range of poles to bedding in packet 4 is due to late open folding, as in packets 2 and 3.

Packet 5

Packet 5 contains an apparently continuous succession of terrigenous strata, of which the lowest are mudstone of unit tm2 (Fig. 2). Upward-thickening and upward-coarsening sequences of turbidites lie above the mudstone. The stratigraphically higher northern one-half of the packet is a multilayer of thick sandstone and thinner turbidite and mudstone interbeds (Table 1).

Structures in the central northern half of packet 5 are shown in map and section in Figure 11. Orientation data of structural elements, displayed in Figures 12 and 13, are divided among six domains that are delineated in Figure 12. Three sequential fold sets are resolved: nearly recumbent first folds, a set of outcrop-dominating high-frequency second folds that occur locally along the margins of packet 5 and are probably related to motions along packet boundaries, and a third set of open major folds that deform packet 5 and the Chalky Mount fault zone.

First Folds

The earliest deformation in packet 5 is represented by a single major fold and a couple of probably contemporaneous minor folds. The major fold is nearly recumbent (Fig. 11, sections) and was initially close to chevron shape. Its axial surface, folded in younger deformations, dips within 30° of horizontal in diverse directions but chiefly to the south. The upper limb (Fig. 12, domain 5a) is upright and north-dipping and occupies a small region in a synform of the third phase. The lower limb, which constitutes the remainder of packet 5 (Fig. 12, domains 5b-g), is inverted and south-dipping. Minor folds of the first phase are recognized only in the upper limb.

The axial trace of the major first fold (Fig. 11) can be followed west from its eastern intersection with the Chalky Mount fault zone to a point where identification is lost because the fold opens rapidly to the west. Within this interval, a dozen measurements of apical angle at sites where the hinge is exposed range from 52° to 146°; most are between 85° and 120°. The average angle between homoclines of upper and lower limbs is about 100° (Fig. 12d). There is no systematic variation of apical angle along the axial trace, and much of the variability is probably due to later deformation. Near the point where the axial trace loses

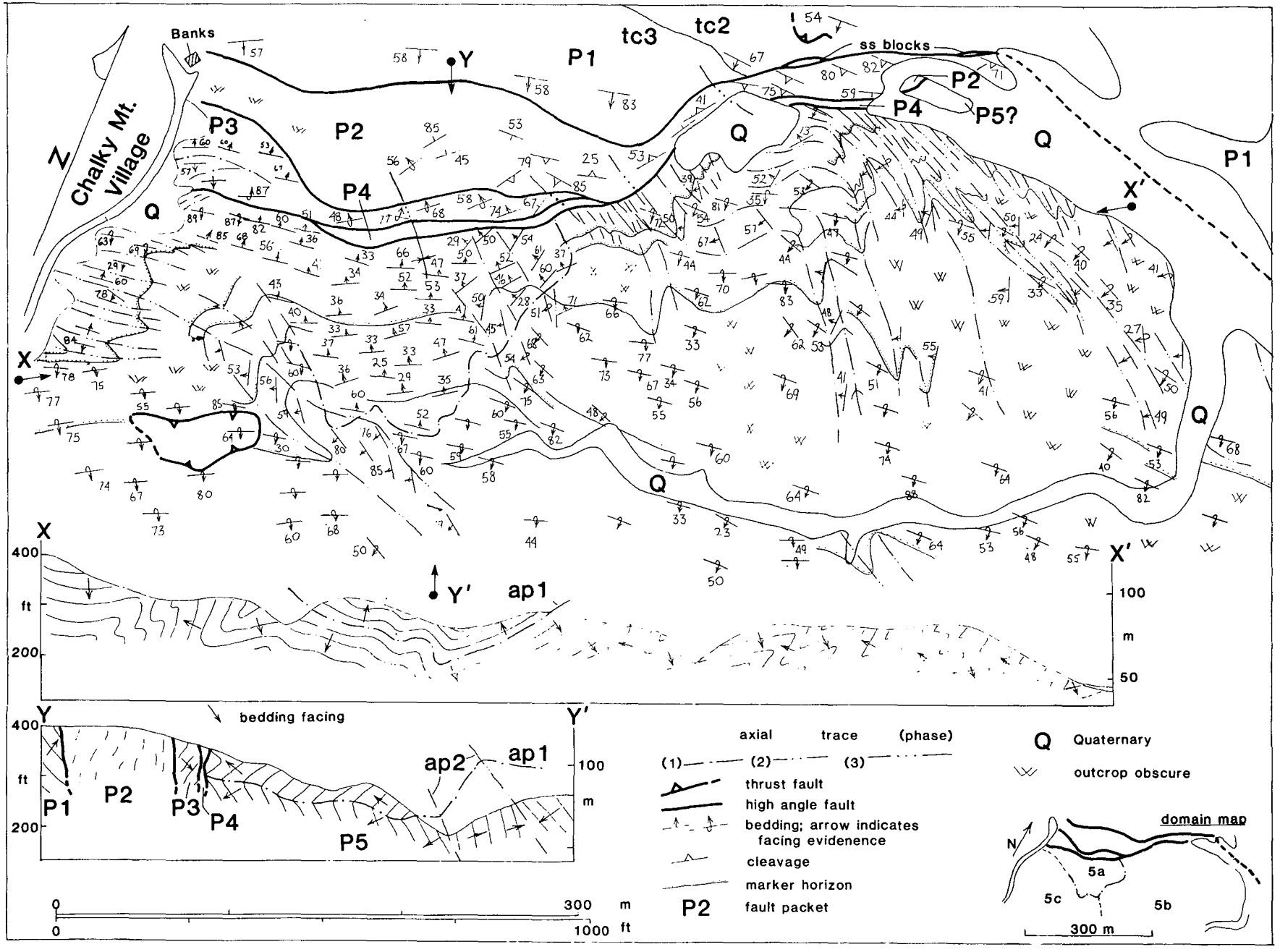

Figure 11. Geologic map and vertical sections of central northern fault packet 5; map location in Figure 3; vertical sections of second folds are diagrammatic, because axes are within ± 30° of reclined; sections can be more accurately viewed as maps of second folds.

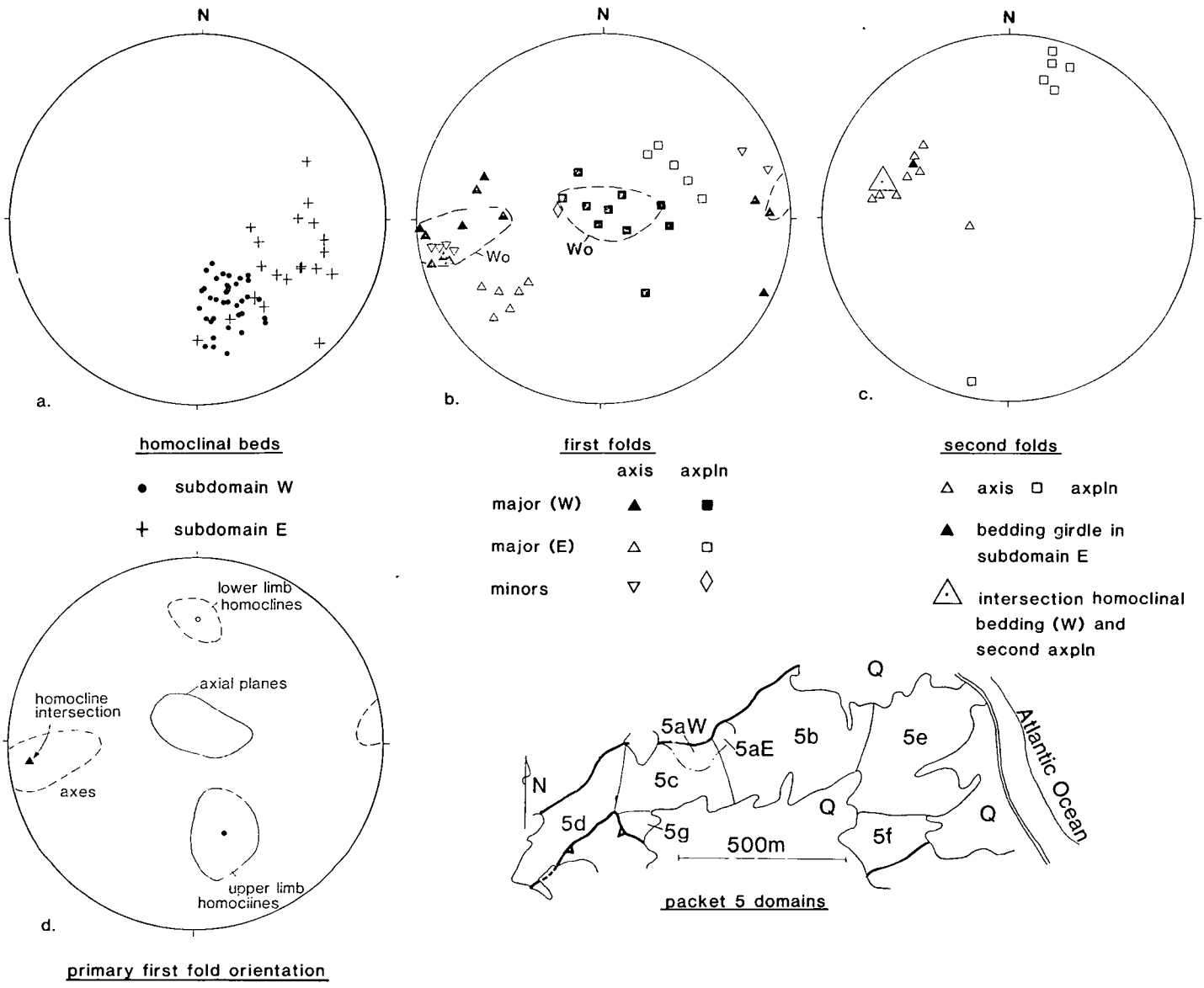

Figure 12. Fold-orientation data for domain 5a, fault packet 1; a: bedding in homoclines ≥2 m on strike in two subdomains, W and E, indicated on domain map; b: first fold data; c: second-fold data; d: reconstructed first fold orientation ranges.

definition, beds of the upper limb steepen west over 10 to 20 m to near-vertical. From this point west, the major fold is gentle (apical angle greater than 150°) and probably has a broad hinge region. The cryptic axial trace where the fold is gentle presumably intersects the Chalky Mount fault zone within Chalky Mount Village.

Later analysis suggests that before second folding, axial planes of first folds dipped ≤20° between west and south and axes plunged shallowly west-southwest. Disruption of a minor fold assigned to the first phase at its contact with the Chalky Mount fault zone (Fig. 14d) indicates that at least late fault movements postdate first folding.

Second Folds

Second-phase deformation in packet 5 created relatively appressed high-frequency folds on the limbs of the early major fold. The second folds, thus, yield conspicuous deformation patterns on an outcrop scale. They form an irregular train of S asymmetry with S and Z parasites on limbs of larger second folds and have widths from 1 to 30 m and apical angles from 14° to 146°, averaging about 60°. Fold width varies with layer thickness and with proximity to the Chalky Mount fault zone. Single surface shapes of second folds are chevronlike in thin-bedded successions, whereas in thick beds they are closer to sinusoidal. Thick beds commonly maintain constant orthogonal thickness around hinges and are rarely faulted. Many folds of thick beds, however, are necked within one metre or so of the hinge on one or both limbs, most commonly on the overturned limb. The fold necks are like features called hinge collapse and are ascribed to kinematic incompatibility of layers of different thickness during chevron folding by Ramsay (1974). As in packet 1, thin interbeds between folded thick beds are commonly detached, translated hingeward, and deformed in tight metre-wide folds of more variable orientation than the host.

Evidence that second folds are super-

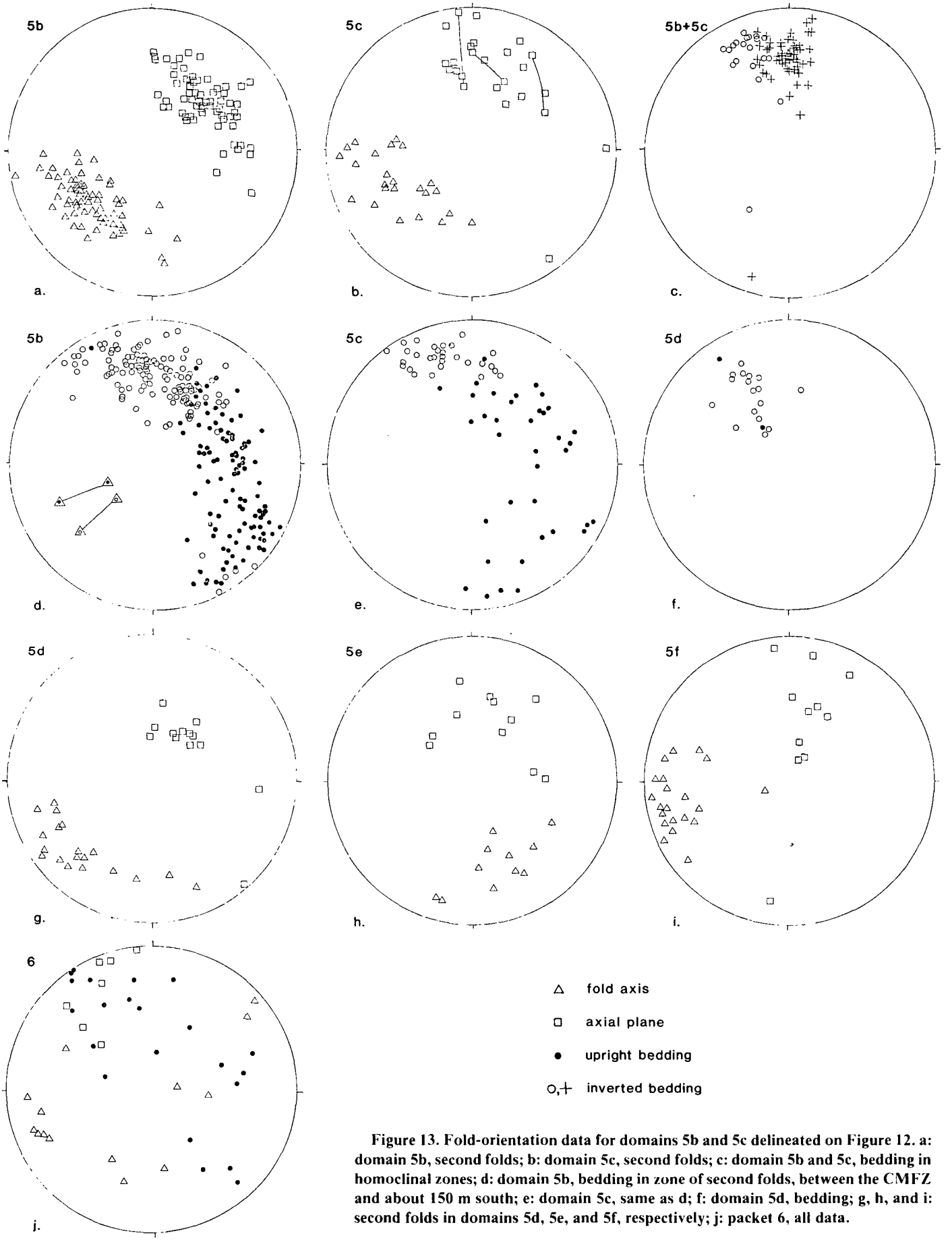

Figure 13. Fold-orientation data for domains 5b and 5c delineated on Figure 12. a: domain 5b, second folds; b: domain 5c, second folds; c: domain 5b and 5c, bedding in homoclinal zones; d: domain 5b, bedding in zone of second folds, between the CMFZ and about 150 m south; e: domain 5c, same as d; f: domain 5d, bedding; g, h, and i: second folds in domains 5d, 5e, and 5f, respectively; j: packet 6, all data.

posed on rather than contemporaneous with first folds is: (1) different distributions of axial planes and axes of the two sets, (2) change of axis orientation and fold facing with more or less constant axial-plane attitude of second folds where they cross the axial trace of the major first fold, and (3) different distribution of upright bedding attitudes in second folds superposed on the inverted limb of the first major fold from that of the upper limb of the first fold (compare Figs. 12c and 13d).

Second folds are concentrated in a belt within 100 to 200 m of the Chalky Mount fault zone in the area of Figure 11. South of the belt of second folds is a subparallel zone of nearly homoclinal beds with only a few second folds (Fig. 11). Their distribution and the dependence of their frequency content on proximity to the Chalky Mount zone imply that second folds are related to motions in the fault zone. Folds considered second phase are also locally exposed south of the homoclinal zone in what may be a belt adjacent to the packet 5–6 fault. Domainal orientation data on second folds given below are from the more thoroughly studied northern fold belt.

Third Folds

Third folds consist of poorly delineated major open folds that deform the Chalky Mount fault zone and at least the northern portion of packet 5. Four third folds can be resolved. The highly approximate locations and trends of their axial traces are shown in Figure 11. The three easternmost axial traces occur in a generally north-closing warp of the Chalky Mount fault zone and a culmination of second folds in packet 5. The western axial trace reflects a south-closing warp of the fault zone and a structural depression of packet 5 in which the upper limb of the major first fold is preserved. The structural culmination of second folds below the covered area of Chalky Mount Village (Fig. 11) may also be a third fold. Third folds have poorly determined axial planes of northwesterly strike and steep dip. Third folds may represent a continuation of second folding after locking of faults in the Chalky Mount zone.

Domain 5a

Domain 5a includes the upper limb and axial trace of the major first fold in the region where the fold is tight enough to allow location of the hinge (Fig. 11). It also includes steeply dipping homoclinal beds, presumably upper limb, that lie farther northwest. The eastern one-third of domain 5a (E subdomain, Fig. 12) is substantially affected by second- and third-phase folds, whereas the western two-thirds (W subdomain) is less refolded. Figure 12a shows that bedding in local homoclines in W forms a shallowly west-plunging partial girdle, whereas that in E occupies a partial girdle about a northwest-plunging axis. Attitudes of the major fold, measured at 16 scattered outcrops of the hinge, are shown in Figure 12b. At some sites, the axial plane could not be determined, and the bisecting plane is used instead. The validity of the substitution is implied by near-parallelism of the two planes ($\leq 15°$) where the axial plane is known and by the similarity of orthogonal bed thickness in both limbs.

Points on Figure 12b enclosed by dashed line (Wo) are first fold elements in areas of subdomain W, where effects of second folding are minimal. Such attitudes may represent the original orientation of the major first fold. This is supported by the approximate colinearity (Fig. 12d) of unrotated first axes (Wo, Fig. 12a) and the intersection of mean homoclinal bedding in the upright limb (subdomain W, Fig. 12a) and in the inverted limb (domain 5b, Fig. 13c). The colinearity also indicates the absence of substantial bulk rotations between domains 5a and 5b during later deformations. Thus, the pre-second phase axis of the first fold plunged shallowly west-southwest. Axial planes within distribution Wo (Fig. 12b) that contain such an axis dip between south and west $\leq 25°$. The initial fold was nearly recumbent.

Second folds in domain 5a differ in atti-

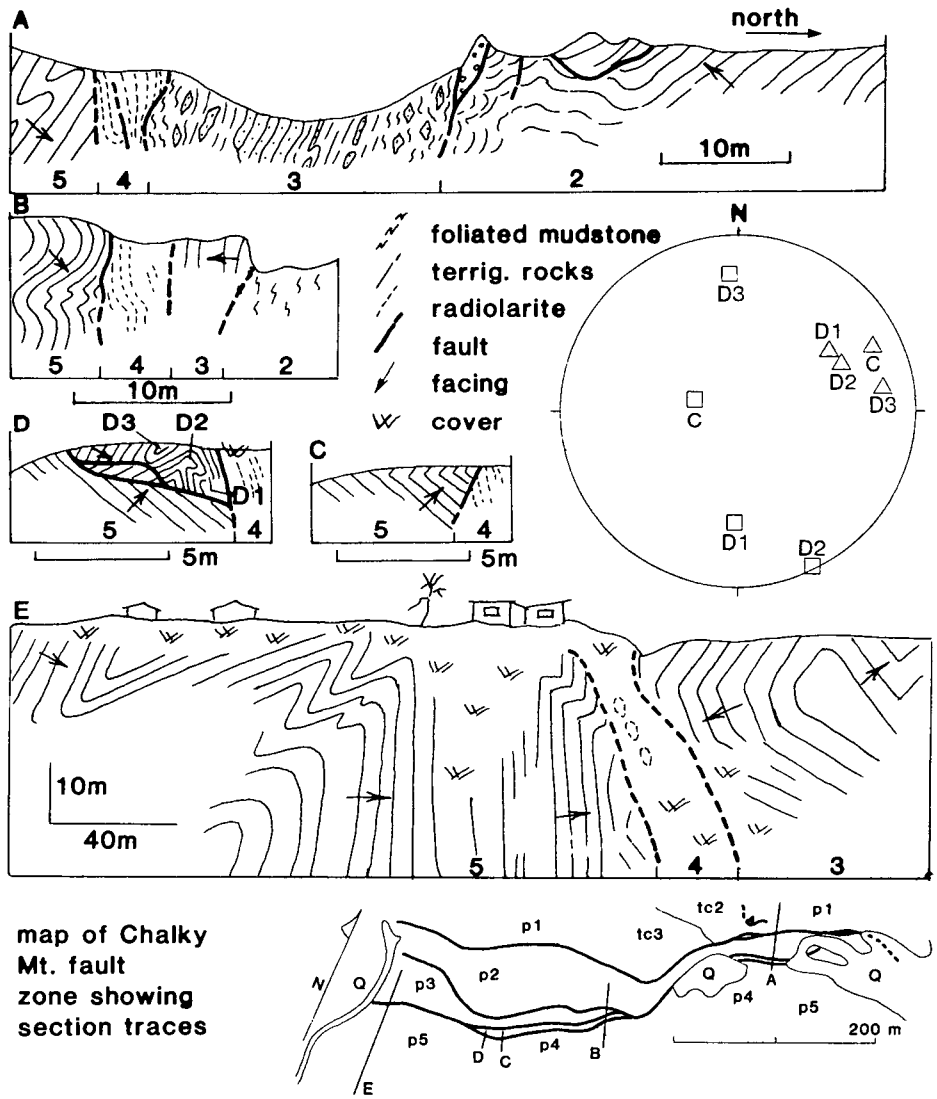

Figure 14. Vertical sections across parts of the Chalky Mount fault zone; fault packets identified by number at bases of sections; orientation data for undisrupted first fold C in section C and superposed folds D1–3 in section D where fold C is deformed.

tude from first folds (compare Figs. 12b and 12c). Most second axes lie close to the intersection of mean homoclinal bedding in subdomain W and the average second axial plane (Fig. 12c). Poles to bedding in subdomain E (Fig. 12a) are partially girdled about the same general axis.

Domains 5b and 5c

These domains (Fig. 11) include folds of the second and third phases superposed on the inverted lower limb of the major first fold near its hinge and, farther south, homoclinal inverted beds. Data presented below are from second folds; characteristics of the macroscopic third folds are then inferred from other information.

The density (axial traces per unit area) of second folds is maximum at the Chalky Mount fault zone and diminishes to near zero 100 to 200 m south of the fault zone. The changes are indicated by mapped axial traces in Figure 11 (somewhat diagrammatically because many small folds near the CMFZ are not mapped) and by comparison of bedding attitudes in the belt of second folds (Figs. 13d, 13e) with that in the homoclinal zone to the south (Fig. 13e). The main change across the belt of second folds is the increasing content of parasitic folds toward the fault zone, but not in orientation or tightness, as will be described fully elsewhere.

Figures 13a and 13b show that axes and poles to axial planes are in northwesterly-striking girdles with ranges of trend around 90° and that the average fold orientation in domain 5b is reclined in a southwest-dipping axial plane but nonreclined in domain 5c. Asymmetry and facing relationships are as follows: (1) most folds are S; (2) S folds are either inverted or upright, whereas Z folds, all parasitic, are upright; and (3) inverted and upright folds have generally different orientation distributions where those with right-pitching axes are upright, those with left-pitching are inverted, and the transition is through a reclined orientation.

Comparison of bedding attitudes in the homoclinal zone (Fig. 13c, all bedding inverted) with those to the north in the belt of second folds (Figs. 13d, 13e) shows that inverted beds throughout domains 5b and 5c have approximately the same orientation ranges. The long limbs of second folds are inverted, whereas the short limbs are commonly upright. The data indicate the second folds developed largely by rotation of short limbs to upright facing from an initial attitude in a south-dipping inverted homocline. The fundamental rotation was counterclockwise or with southeasterly vergence.

Further data on second folds of domains 5a and 5b and a kinematic interpretation of their development will be presented in a subsequent paper. Three points to be made are: (1) the position of the belt of second folds and its change in frequency content argue that the folds originated by displacements of packet 5 relative to its northern boundary; (2) the displacement gradient can be interpreted as quasi-homogeneous simple shear in the northern 100 m or so of packet 5 due to left-oblique slip (pitching east-southeast, 40°) on the southern strand of the CMFZ; and (3) the variability in orientation of second-fold elements is partly primary and partly due to homoaxial third folding.

The principal evidence for third folds comes from the harmonic inflection of faults of the CMFZ and planar structures in packets 2, 3, and 4 (Fig. 10). These inflections represent open folds with northwest-trending axial traces. Thus, packet 5, or at least part of it bordering the fault zone, must be involved in these folds that developed after cessation of slip on the three southern faults. Because the attitudes of second and third axial planes have similar strikes, the third folds may record continuation of earlier motions after the faults became locked.

Domain 5d

Domain 5d (Fig. 12) occupies the poorly exposed western quarter of packet 5, and exposed beds largely make up inverted homoclines, except in southwestern domain 5d, where a set of tight and laterally continuous folds occurs. It is probable that the nearly homoclinal zone of domain 5d is a westward continuation of that of domains 5b and 5c. The mean homoclinal strike in domain 5d, however, is slightly more northeasterly (Fig. 13f) than that of domain 5c (Fig. 13c), and the range of dips is greater. Unlike the homoclinal zone in domains to the east, that of domain 5d apparently contacts the Chalky Mount fault zone. Moreover, there is no evident change in bedding attitude with proximity to the fault zone, although the data are meager.

Occasional minor folds occur in the homoclinal zone, but none seems to be in a continuous wave train. They are chiefly S, left-pitching, and inverted (Fig. 13g), thus following the geometric relationships of folds in domains 5b and 5c. The axes in domain 5d are more easterly-pitching than those of 5b and 5c (Figs. 13a, 13b), in agreement with the intersection of average homoclinal bedding (Fig. 13f) and axial planes (Fig. 13g). Therefore, minor folds of homoclinal zone in domain 5d are probably contemporaneous with second folds to the east. The difference in orientation between second folds of domain 5d and those of domains 5b and 5c is at least partly primary but may also reflect rigid rotation about a near-vertical axis.

The question arises why a zone of concentrated second folds does not occur between the nearly homoclinal beds and the Chalky Mount fault zone in domain 5d. Possible explanations are: (1) domain 5d may occupy a region like that of the third-phase synform in the area of Figure 11, where second folds are less abundant; (2) a former zone of concentrated second folds in domain 5d may have been faulted off by completely brittle postfolding displacement on the southern fault of the Chalky Mount zone; or (3) a fold zone may never have formed, perhaps because homocline strikes in domain 5d are close to parallel with those of the fault so that shear strain in the wall involved less cross-layer shortening than it did farther east.

The structural zone of minor folds in the southwestern corner of domain 5d may be continuous at depth with folds in domain 5g (Fig. 2). Their origin may be similarly related to motions at the boundary of packets 5 and 6.

Domain 5e

Domain 5e (Fig. 13h) includes the eastern continuation of the zone of inverted homoclinal beds and the second-fold belt from domain 5b. Minor folds in domain 5e, probably all second folds, have a large range of axial trends and, like folds in domain 5b, upright folds have right-pitching axes and inverted, left-pitching. The trend of reclined folds in domain 5e is about 45° south of that of domain 5b, perhaps indicating different initial bedding orientation and(or) rigid rotation about a near-vertical axis with respect to domain 5b.

Domain 5f

Domain 5f (Fig. 12), southeasternmost in packet 5, contains the following north-to-south sequence of structural features: homoclinal zone, fold zone, thrust nappe, and steeply dipping fault southern boundary to packet 6 (section AA′, Fig. 2).

The homoclinal zone is composed of steeply dipping, chiefly inverted beds of easterly strike. Such beds are almost certainly in continuous section north to domain 5e and west on strike to those of domain 5b. The zone of folds that apparently represents a southern marginal fold belt of packet 5 includes a major overturned anticline that exposes the lowest stratigraphic unit, tm2, in packet 5. The minor folds (Fig. 13i) verge to the north and have shallowly west-plunging axes. Their wavelengths vary from 3 to about 30 m; asymmetries are S. Because the short limbs are upright like folds north of the homoclinal zone, these folds are probably second folds imposed on the inverted southern limb of the major recumbent first fold. If this interpretation is correct, the inverted limb of the first fold is nearly planar over a stratigraphic thickness exceeding 400 m and constitutes all of packet 5 except for domain 5a. The southern boundary of packet 5 is a steep irregular fault that juxtaposes gently folded sandstones of packet 6.

Domain 5g

Domain 5g includes a group of second folds that lie south of the homocline zone of domain 5e and below the thrust that here forms the packet 5–6 boundary. These folds may occupy a southern fold belt in packet 5 together with folds in domains 5d and 5f and are perhaps related to relative motions between packets 5 and 6. Orientation data from domain 5g are too spotty to attempt kinematic interpretation.

Packet 6

Packet 6 consists largely of coarse-grained terrigenous sandstone that is commonly rich in solid hydrocarbons (Table 1). Two discrete outcrop areas intervened by alluvium are included in packet 6. Although both are characterized by hydrocarbon-rich coarse sandstone (Table 1), it is hard to prove that they expose the same structural unit.

The western tract of packet 6 lies above packet 5 with south-dipping thrust contact. More than 200 m from the thrust trace, packet 6 contains a train of open-to-closed upright folds of wavelength of 50 to 100 m. Axes of most of these folds plunge shallowly west-southwest, and their axial planes are near vertical (Fig. 13j). Closer to the thrust trace, folds take on different orientations, wherein axes seem to define a broad southeast-dipping girdle. Three of the four measured axial planes of such folds are approximately parallel to the axis girdle. Although the data are too meager to be conclusive, the fold element pattern of Figure 13j suggests rotation of early formed axes (shallowly west-southwest and east-northeast-plunging) toward an elongation direction with northwesterly component during thrusting, as formalized by Escher and Watterson (1974). The folds away from the thrust trace and presumably higher in the nappe than those near the trace are presumably unaffected by the thrust motions. The higher folds may have been above a basal zone of displacement gradients in the nappe and so escaped reorientation, as has been demonstrated in other nappes by Williams (1978).

The eastern tract of packet 6 (section AA', Fig. 2) contains open-to-close upright folds. Its contact with packet 5 is vertical to steeply south-dipping and is locally irregular in strike and dip. The boundary is abrupt, and fault rocks are absent.

CHALKY MOUNT FAULT ZONE

Faults

The Chalky Mount fault zone is composed of four high-angle faults and the intervening narrow lenticular packets 2–4 in a belt 10 to 100 m wide (Figs. 3, 11). Packet-bounding faults of the CMFZ strike between east and N50° E and dip within 25° of vertical, chiefly to the south (Fig. 14). Their nonplanarity is due to pinch and swell of internal packets and to northwesterly-trending open folds (Fig. 11) that are equivalent to third folds in packet 5.

As observed in excavations and a few natural exposures, faults of the CMFZ are generally discrete surfaces with wall rocks that have undergone some degree of deformation related to fault slip. At least locally, the faults have polished faces (now weathered) and millimetre-wide striae. The existence of foliated, disrupted, and locally folded wall rocks indicates that displacements were distributed across zones of finite width.

Direct net-slip indicators are meager. Striae on the packet 1–2 fault plunge between east and south. Another indicator is provided by several blocks or micropackets of very coarse-grained sandstone exotic to adjacent wall rocks within the same fault near its easternmost exposures (Fig. 11). The block faces and their internal lamination are discordant to layering and foliation in the fault walls. The exotic blocks are lithologically like the distinctive gritty beds of unit tc3, packet 1, that abuts the packet 1–2 fault some 100 to 200 m west (Figs. 2, 11). If such blocks are correctly correlated, displacement on the northern fault of the CMFZ is south wall down and(or) east, in harmony with striae directions.

Disrupted Rocks of Packet 2

Strongly disrupted sandstone beds and spaced cleavage (Fig. 5f) occur in eastern packet 2 (Figs. 2, 11), chiefly near the northern packet margin, and probably formed during relative motion of packets 1 and 2. The strongly disrupted rocks grade abruptly to more coherent ones; sandstone blocks all appear to have been derived by tectonic fracturing and dispersion of beds within packet 2.

Cleavage is anastomosing and spaced by microlithons 0.1 to 5 mm thick. It parallels axial planes of tight microfolds of sedimentary laminae and is itself locally folded homoaxially with the laminae. Sandstone blocks, 3 to 60 cm long, are mostly tabular parallel to internal lamination. The largest faces represent original bed contacts. Block tips are commonly faceted or lensoid, indicating failure by shear fracture or by initial boudinage, perhaps both. Only a few true boudins (necked connectors between blocks) exist, and these occur in relatively thin-bedded and probably muddy sandstone. Where cleavage is widely spaced and indistinct, sandstone blocks are concentrated near local horizons, evidently former bedding, and have block-gap ratios between 0.1 and 1. Where cleavage is more closely spaced, blocks are more widely dispersed and hard to relate to original bedding. Tabular block faces are generally aligned with one another and with the average attitude of local cleavage. No striae occur on the tabular faces, whereas facets at angles to the tabular faces and to average nearby cleavage are locally striated. Sandstone blocks show no obvious shape lineation or internal foliation.

The proximity of the disrupted rocks of packet 2 to the northernmost fault of the Chalky Mount zone indicates disruption probably occurred during relative motion of packets 1 and 2. The normals to the tabular block faces and cleavage are interpreted to record the shortening direction due to plane shear strain in the fault wall and the boudins to indicate the intermediate strain-axis attitude. Thus, knowing the orientations of the principal strain components and the

shear (fault) plane, a solution for the shear direction (net slip) can be obtained: left-oblique slip pitching 20° to 30° east. The validity of this direction is indicated by (1) the displacement of sandstone blocks thought to be correlated with unit tc3, (2) orientation of fault-plane striae within ± 60° of this direction, and (3) the similarity of interpreted displacement on the packet 4–5 fault.

Packet 1

Beds and folds of the main set are slightly to moderately broken locally for about 10 m out from the northernmost fault (Fig. 14a). Stratigraphic offsets are as great as a few metres in the zone of broken folds, but slip directions are uncertain. The broken folds indicate that at least some motions on the northern fault of the CMFZ postdated the main fold set.

Packet 4

The fault that separates packets 4 and 5 (Fig. 14b) occupies a zone of fractured mudstone 10 to 15 cm wide between sharp boundaries with friable sandstone of packet 5 on the south and unfractured mudstone laminated by varied concentrations of radiolaria of packet 4 on the north. The zone of fractured rock contains scattered grains and nests of quartz sand and equant masses of mudstone like that of packet 4, about which the fractures sweep. The fractured rock probably developed in packet 4, and quartz was plucked off the wall of packet 5 and mixed inward during displacement. Radiolaria in packet 4 apparently are undeformed.

Packet 5

Figures 14c and 14d illustrate the disruption of a fold at the southern fault of the CMFZ. Section C shows an intact recumbent minor fold in the upright limb of the major first fold of packet 5. The minor fold is assumed to be a first fold by virtue of its similar attitude to the major fold. Twenty metres west (Fig. 14d), the recumbent minor fold is faulted along much of its axial surface and above, and its upper limb is refolded. The superposed folds of beds are approximately homoaxial with the first fold.

An obvious difference in sections C and D (Fig. 14) is the attitude of the southern fault of the CMFZ, south-dipping where the first fold is intact and north-dipping where it is disrupted. The relationships are interpreted as follows: the north-dipping fault in section D represents a local asperity in the fault's north wall, and the first fold in the south wall was deformed as it was displaced across the asperity. The first folds, therefore, are taken to be of pre-fault generation.

STRUCTURAL SUMMARY

The basal complex of Barbados at Chalky Mount and vicinity consists of six fault-bounded packets of east-northeast strike and generally steep dip. Packet-bounding faults are generally discrete slip surfaces, but deformation in fault walls indicates that the youngest displacements on some were distributed in zones as wide as 200 m. All packets are composed of deformed sedimentary rocks, five of terrigenous strata and the sixth of hemipelagic. There is no evidence of former stratigraphic continuity among beds of any of the six packets.

Rocks within fault packets have undergone one or more phases of tectonic deformation. Table 2 organizes the sequential deformations of each packet with respect to final motions on packet-bounding faults or, equivalently, cessation of interpacket slip. Table 2 also compares deformation phases within and among packets by trend of shortening directions, taken as the bearing (nonvectoral) of the normal to mean axial plane of the folding phase.

In packet 1, beds underwent major first deformation before and(or) during motions on the packet's southern boundary. The first deformation consists of a pervasive train of folds (D1) that are upright or overturned to the north. It also includes local structures (D1*): imbricated thrust slices and thrust nappes, both of which may contain tectonic broken formation, and folds that are either early or late with respect to the main fold train. D1* folds verge north-northwest, and transport on thrusts was probably in the same direction. D1 and D1* structures are homoaxial about shallowly west-southwest–plunging axes. The D1* structures probably represent local zones of substantial rotation during progressive deformation. Packet 1 contains two recog-

TABLE 2. RELATIVE TIMING OF DEFORMATION EVENTS

t	1	2	3	4	5	6
Early	D1 (NNW-NNE) D1* (NNW-NNE)	Tight fold (N ·)	Close to tight folds (N ·)	Folds (N ·)	First near recumbent folds	folds (N ·)
Contemporaneous	Disruption at p1-2 fault	Local foliation and disruption	Fold modification?	Brecciation, internal faulting	Second folds (NNE–ENE) Local deformation of first fold at p4-5 boundary (N ·)	
Post		Open folds (NE ·)	Open folds (NE ·)	Open folds (NE ·)	Third folds (NE ·)	
?	D2 (NW)					Thrust salient and fold axis girdle (NW?)

Note: Events in packets 1–6, related to timing (t) of last motions on packet-bounding faults; associated shortening trends are in parentheses.

nized second-phase folds (D2), both open and with northeast-trending axial traces. The two folds may represent cryptic packet-wide structures that can be inferred statistically, or they may be local and related to slip on an intrapacket thrust. The timing of D2 with respect to interpacket motions is unknown.

The early structures in packets 2–4 are west-trending and were generated before and(or) during motions of faults of the Chalky Mount zone (Figs. 2, 11, 14). Broken formation and reorientation of early structures in part of packet 2 were caused by late left-oblique slip on its northern boundary fault. Packets 2–4 and at least the three southern faults of the CMFZ are warped by several open folds with northwest-trending axial traces. Such folds, shown as third phase with respect to packet 5 on Figure 11, are younger than last interpacket displacements.

Early deformation in packet 5 is represented mainly by a major, nearly recumbent, fold of amplitude that apparently exceeds packet width, about 0.5 km. The early fold is cut at high angles by both packet-bounding faults. A width of 100 to 200 m of the northern wall of the eastern two-thirds of packet 5 is strongly deformed by displacements related to late motions along the packet 4–5 fault. The displacement gradient created synfault northwest-trending second folds that are superposed on the early recumbent major fold. The second folds are interpreted (R. C. Speed, unpub. data) as products of left-oblique simple shear with a slip vector plunging approximately 40°E. Third folds that are homoaxial with the second folds deform the northern wall of packet 5 and at least part of the CMFZ to the north of it. The third folds are probably products of the same motions represented by the second folds but formed after the faults locked.

For the most part, packet 6 contains early folds that are probably in a continuous homoaxial train and have steeply dipping axial surfaces. Northwestern packet 6 is an exception because it overlies packet 5 on a south- to southwest-dipping thrust and contains reoriented early folds. The partial girdle of early fold axes in the anomalous area suggests northwest transport on the thrust. It is not clear whether the thrust is part of the primary northern boundary of packet 6 or a younger feature.

INTERPRETATION OF EARLY STRUCTURES

All six packets have early (Table 2) deformation features, among which there are common elements. First, the earliest layer deformations in each packet are almost entirely tectonic. Slumps are rare. Although intrastratal soft-state deformation is commonplace, the strata of Chalky Mount and vicinity apparently were deposited at places that permitted little resedimentation of layer successions. Second, the early deformation in each packet was the major one, both in pervasity and, probably, in total shortening. Third, early fold sets have similarities in orientation. The shortening trends (Table 2) in each packet, with the possible exception of packet 5, are approximately parallel to one another and normal to packet boundaries. Moreover, axes of unrefolded early folds are all shallowly plunging between west and southwest. This direction lies in or close to packet-bounding fault surfaces.

The original dip direction of the axial plane of the nearly recumbent major early fold in packet 5 is uncertain between south and west. If the axial plane had dipped west, the fold would have been reclined. I consider it more probable that the axis of the packet 5 first fold was normal to the dip of the axial plane, as with other early folds at Chalky Mount. The rationale suggests an initial south-dipping axial plane and a shortening trend in consonance with early deformations of other packets.

A fundamental relationship evidently exists between the fault packet architecture and early deformation within packets. Two possible explanations are as follows: (1) packet-bounding faults are surfaces of accretion, and the early structures are products of shortening during accretion on such surfaces; and (2) packet-bounding faults cut an earlier deformed depositional or tectonic succession and are controlled in orientation by strike of the earlier structures. The second explanation seems unlikely from studies at Chalky Mount and northeastern Barbados as a whole (Speed and Larue, 1982) because (1) different lithic suites (terrigenous, hemipelagic, debris flow) of the basal complex all occupy discrete fault-bounded packets (about 30 recognized to date); (2) nowhere are rocks of different lithic suites deformed together within a packet; (3) the strongly contrasting lithotypes of the terrigenous and hemipelagic suites are age overlapping, perhaps throughout the whole of the Eocene. Therefore, an origin of the packets and their early deformations by accretion is proposed.

The accretionary process is visualized as follows. Strata on a subducting ocean floor within a depth interval between the sea bottom and a décollement were driven against the surface that was the front of the accretionary prism. The surface may have been subvertical or shallowly arcward-dipping. The accreting sediment was shortened with horizontal trend normal to the buttress, with or without rotation about nearly horizontal axes in the plane of the buttress. The width and time-dependent properties of the deformation zone are unknown and would have varied with thickness and stiffness of particular accreting sediment packets. At some stress- or strain-related threshold, the deforming tract of sediment faulted on its seaward side, completing the transfer from ocean floor to prism, and the seaward fault became the new accretionary surface. All sediment on the subducting plate may not have been transferred to the accretionary prism at the same structural level because (1) sediment below a time-variable décollement may have been transported well under the prism or farther, and (2) a time interval may have existed between the development of a seaward fault on an accreted packet and the attachment of strata to the newly created accretionary surface.

Given the postulated process, differences among early structures at Chalky Mount imply that packets were not transferred identically. Packet 1 underwent local north-verging rotations, but early-phase rotations have not been detected in other packets. Axial planes are nearly parallel to accretionary surfaces in packets 1, 2, 3, and 6, whereas they have high inclinations to such surfaces in packets 4 and 5. These differences may reflect different conditions at the buttress or on the décollement, different properties of the accreting strata, and so on. Many other unknowns infect the interpreted process. One is how much of the early deformation actually occurred after transfer of the packet to the prism as a soft, deformable buttress. Second, there is no evidence for the initial dip, hence amount of intraprism rotation, of the accretionary sur-

faces. Third, the stacking sequence among accreted packets is unknown. Fourth, the northerly shortening is obviously hard to understand if the accretion was due to convergence like that of today's east-west Atlantic-Caribbean system. Explanations for this discordance (Speed, 1981) are: (1) the older or arcward reaches of the accretionary prism were created in an arc system that was differently oriented from the Neogene Lesser Antilles, and (2) there has been large tectonic rotation of early structures from original north-south strike. The first seems more probable.

INTERPRETATION OF LATER STRUCTURES

Later structures are superposed on early ones and are classed with respect to last motion (syn, post, or unknown) on packet-bounding faults in Table 2. All are nonpervasive, and all are related to late slip on packet-bounding and other faults, with the possible exception of D2 folds in packet 1.

The most conspicuous of the later structures is the belt of second folds in the northern wall of packet 5. These folds and broken formation in eastern packet 2 are interpreted (R. C. Speed, unpub. data) to be related to left-oblique slip on the packet 4–5 and 1–2 boundaries, respectively. Third folds in packet 5 fold the fault-contemporaneous second folds and the southern strands of the Chalky Mount fault zone. The homoaxiality of second and third folds in packet 5 suggests the two phases are related and spanned the cessation of interpacket slip.

The D2 phase of packet 1 cannot be timed within the sequence of Table 2, nor is it certain whether D2 comprises only the two recognized folds or is pervasive in packet 1. If D2 is local, it is probably related to slip on one or more intrapacket faults (for example, thrust ℓ, Fig. 4) and may reflect a component of right slip. An alternative argument, however, suggests that D2 is pervasive. Major open folds with northeast-striking axial planes (like D2) deform the intermediate tier of nappes (Fig. 1b) and the décollement below it (Speed, 1981). If such folds and D2 are synchronous, the D2 phase is post-fault because the décollement of the intermediate nappes appears to be younger than interpacket motion of the basal complex.

If the early structures of the basal complex were indeed generated by flattening against accretionary surfaces, the fault-related later structures must represent products of reactivation of such surfaces. In particular, the left-oblique slip on the packet 1–2 and 4–5 boundaries is demonstrably younger than the early structures. Thus, the later structures are probably intraprism deformations because they seem to represent gross departures from early kinematics. Although the early structures can be interpreted as entirely related to accretion, it is not clear whether they were generated completely during packet transfer or whether they also include components of quasi-coaxial progressive shortening within the prism.

DEFORMATION CONDITIONS AND MECHANISMS

Early structures at Chalky Mount can be interpreted to have formed brittlely on a grain-size scale and in moderately cohesive sedimentary rocks. The main observations are that early folding created wave trains with at least 30% to 40% shortening in packet 1 and that in all packets, folding occurred in layer successions with large apparent flexural rigidity contrasts and maintained orthogonal layer thicknesses of sandstone beds. The existence of early thrust ramps and broken formation implies the rocks had strength at this stage.

The prevalence of intrastratal fluid-escape structures and the paucity of sandstone dikes at Chalky Mount suggest that sandstones lost considerable pore fluid by synsedimentary mechanisms before the onset of tectonic deformation. The porosity of mudstones is now very low (5% to 20%), implying substantial volume loss, but the timing of the porosity decrease is uncertain.

Displacements in the early deformation were taken up probably in part by interlayer sliding, especially between mudstone and thick sandstone beds. There is, however, no evident deformation of grain shapes in sandstones, and mudstones have no megascopic cleavage related to early structures. Therefore, displacements within layers were probably taken up by intergrain sliding (Borradaile, 1981). Because this is a frictional mechanism, I infer the existence of high pore-fluid pressure, but not overpressure. The maintenance of layer cohesion with large intergrain sliding implies that strong seals existed to prevent fluid escape during deformation.

Later structures created by reactivation of packet boundaries differ from early ones by the existence of cleavage in mudstone and fragmentation of sandstone beds. Sandstones failed mainly by faulting and jointing, but apparently only rarely by ductile boudinage.

Structures of all tectonic phases at Chalky Mount and, in fact, in the upper 4 km of the basal complex of Barbados evolved in a distinctly nonmetamorphic environment. The rocks have not passed through great tectonic depths. Therefore, if advective flow exists within the structural high (Cowan and Silling, 1978) of the Barbados accretionary prism, the transport has not been large.

ACKNOWLEDGMENTS

This work was supported by Petroleum Research Foundation Grant No. 12669-AC2.

REFERENCES CITED

Baadsgaard, P. H., 1960, Barbados, W. I.: Exploration results 1950-1958: International Geological Congress, 21st, Report, pt. 18, p. 21–27.

Biju Duval, B., Mascle, A., Montadert, L., and Wanneson, J., 1978, Seismic investigations in the Colombia, Venezuela and Grenada basins, and on the Barbados ridge for future IPOD drilling: Geologie en Mijnbouw, v. 57(2), p. 105–116.

Borradaile, G. J., 1981, Particulate flow of rocks and the formation of cleavage: Tectonophysics, v. 72, p. 305–321.

Chase, R. L., and Bunce, E. T., 1969, Underthrusting of the eastern margin of the Antilles by the floor of the western North Atlantic Ocean and the origin of the Barbados ridge: Journal of Geophysical Research, v. 74, p. 1413–1420.

Cowan, D. S., and Silling, R. M., 1978, A dynamic scaled model of accretion at trenches and its implications for the tectonic evolution of subduction complexes: Journal of Geophysical Research, v. 83, p. 5389–5396.

Douglas, R. C., 1961, Orbitolinas from Caribbean islands: Journal of Paleontology, v. 35, p. 475–479.

Escher, A., and Watterson, J., 1974, Stretching fabrics, folds, and crustal shortening: Tectonophysics, v. 21, p. 225–231.

Hudleston, P. J., 1973, Fold morphology and some geometrical implications of theories of

fold development: Tectonophysics, v. 16, p. 1–46.
Mesollella, K. J., Sealy, H. A., and Matthews, R. K., 1970, Facies geometries within Pleistocene reefs of Barbados, West Indies: American Association of Petroleum Geologists, Bulletin, v. 54, p. 1899–1917.
Moore, J. C., Biju Duval, B., and others, 1982, Offscraping and sediment subduction at the deformation front of the Barbados Ridge: Results from Leg 78A, DSDP: Geological Society of America Bulletin, v. 93, p. 1065–1077.
Peter, G., and Westbrook, G. K., 1976, Tectonics of the southwestern North Atlantic and Barbados Ridge complex: Bulletin of the American Association of Petroleum Geologists, v. 60, p. 1078–1106.
Powell, C. M., 1979, A morphological classification of rock cleavage: Tectonophysics, v. 53, p. 21–34.
Ramsay, J. G., 1967, Folding and fracturing of rocks: New York, McGraw-Hill, 390 p.
1974, Development of chevron folds: Geological Society of America Bulletin, v. 85, p. 1741–1752.
Senn, A., 1940, Paleogene of Barbados and its bearing on the history and structure of the Antillean-Caribbean region: Bulletin of the American Association of Petroleum Geologists, v. 24, p. 1548–1610.
1948, Die Geologie der Insel Barbados B.W.I. und die Morphogenese der Umliegenden marinen Gross formen: Eclogae Geologicae Helvetiae, v. 41, p. 199–221.
Speed, R. C., 1979, New views on the geology of Barbados: Fourth Latin American Geological Congress, Trinidad, 1979, Transactions (in press).
1981, Geology of Barbados: Implications for an accretionary origin: Oceanologica Acta, Actes 26th Congrès International de Géologie, Paris, 1980, p. 259–265.
Speed, R. C., and Larue, D. K., 1982, Barbados: Architecture and implications for accretion: Journal of Geophysical Research, v. 87, p. 3633–3643.
Vaughan, T. W., and Wells, J. W., 1945, American old and middle Tertiary larger foraminifera and corals: Geological Society of America Memoir 9, 175 p.
Westbrook, G. K., 1975, The structure of the crust and upper mantle in the region of Barbados and the Lesser Antilles: Geophysical Journal, v. 43, p. 1–42.
Westbrook, G. K., Bott, M.H.P., and Peacock, J. H., 1973, Lesser Antilles subduction zone in the vicinity of Barbados: Nature, v. 244, p. 118–120.
Williams, G. D., 1978, Rotation of contemporaneous folds in the X direction during overthrust processes in Finnmark, Norway: Tectonophysics, v. 48, p. 29–40.
Woodcock, N. H., 1976, Structural style in slump sheets: Ludlow Series, Powys, Wales: Geological Society of London Quarterly Journal, v. 132, p. 399–415.

MANUSCRIPT RECEIVED BY THE SOCIETY JULY 27, 1981
REVISED MANUSCRIPT RECEIVED NOVEMBER 30, 1981
MANUSCRIPT ACCEPTED DECEMBER 2, 1981

Printed in U.S.A.